



Universität Stuttgart

Institute of Construction Materials
Fastening Technology Department
University of Stuttgart
Pfaffenwaldring 4
70569 Stuttgart, Germany

Phone
+49 711 685-63957
Fax
+49 711 685-62285

Coupled thermo-mechanical inelastic analysis of reinforced concrete flexural members subjected to fire loads

By:

Hitesh Lakhani

Akanshu Sharma

Jan Hofmann

Research Report No: E16/01-C/01
Report Date: 04.04.2016

This report contains 53 pages



Contents:

List of Figures:.....	3
List of Tables:.....	5
Abstract.....	7
1 Introduction.....	9
2 Brief Literature Review:.....	13
2.1 Concrete at Elevated Temperature.....	13
2.2 Experiments on RC beams under fire.....	14
3 Proposed approach:.....	21
3.1 Basic assumption:.....	21
3.2 Thermal Analysis.....	22
3.3 Moment Curvature Analysis.....	23
3.3.1 Temperature dependent Stress – Strain relationship for Concrete.....	24
3.3.2 Temperature Dependent Stress – Strain relationship for Reinforcement.....	25
3.3.3 Generation of moment-curvature characteristics.....	27
3.4 Nonlinear Static Analysis.....	30
4 Validation against experiments.....	33
4.1 Moment Curvature at Ambient Temperature.....	33
4.1.1 Espion and Halleux [38].....	33
4.1.2 Srikanth, Kumar and Giri [39].....	35
4.2 Nonlinear Static Analysis at ambient temperature to obtain load-deflection behaviour.....	36
4.2.1 Pam, Kwan and Islam [40].....	37
4.2.2 Au and Bai [42].....	38
4.3 Nonlinear Static Analysis Approach during fire.....	39
4.3.1 Beam I: Dotreppe [14].....	39
4.3.2 Beam II: Lin, Gustaferro and Abrams [15].....	43
5 Summary and Conclusion.....	47
6 Bibliography.....	49



List of Figures:

Figure 1 Structural collapses due to fire [1].....9

Figure 2 Variation of compressive strength of NSC with rise in temperature [6,10,12,13,11] 13

Figure 3 Variation of Modulus of Elasticity of NSC with temperature [10,11]..... 14

Figure 4 Variation of strength and modulus of elasticity of reinforcement bars with temperature [11]..... 14

Figure 5 Loading and cross-section details of beams reported by Dotreppe [14] 15

Figure 6 Experimental and numerical results of Dotreppe [14] 15

Figure 7 Loading arrangement on beams tested by Lin et al [15] 16

Figure 8 Load distribution and exposure on beams tested by Lin et al [16] 16

Figure 9 Crack pattern in beams tested by Lin et al [16]..... 17

Figure 10 Fire resistance comparison for FT and TF paths [17] 17

Figure 11 Specimen details and variation of furnace temperature for Shi et al. [18]..... 18

Figure 12 Deflection-time for beams tested by Dwaikat and Kodur [19] 18

Figure 13 Spalling in NSC and HSC beams under design fire exposure [19] 19

Figure 14 Deflection time for beams tested by Choi and Shin [20] 19

Figure 15 NSC and HSC beams at failure [20] 19

Figure 16 Thermal properties of concrete23

Figure 17 Temperature dependent stress strain curve for concrete in compression [26]24

Figure 18 Stress strain curve for reinforcing steel26

Figure 19 Flowchart for moment-curvature analysis29

Figure 20 Computed and experimental moment - curvature for beam N0-D-1.234

Figure 21 Computed and experimental moment - curvature for beam N0-D-1.434

Figure 22 Computed and experimental moment - curvature for beam N0-S-1.434

Figure 23 Computed and experimental moment - curvature for beam U135

Figure 24 Computed and experimental moment - curvature for beam U236

Figure 25 Computed and experimental moment - curvature for beam U336

Figure 26 Cross Section details and loading arrangement (Pam et al., [41]).....37

Figure 27 Computed and experimental Moment – Deflection curves for beam B2 & B837

Figure 28 Load - deflection response for beam B138

Figure 29 Load - deflection response for beam B238

Figure 30 Reinforcement details of beams tested by Dotreppe [14]39

Figure 31 Variation of mechanical properties of reinforcing steel with temperature [14].....39

Figure 32 Predicted temperature contours under ISO834 standard fire40

Figure 33 Comparison of temperature variation of central reinforcement40

Figure 34 Moment curvature variation for Beam I41

Figure 35 Variation of k1 factor for Beam I.....41

Figure 36 Load - deflection response at various time during fire exposure for Beam I42

Figure 37 Deflection – time response comparison for Beam I42



Figure 38 Loading arrangement for Beam II [15]	43
Figure 39 SAP2000 Model for Beam II.....	43
Figure 40 Average temperature of bottom reinforcement of Beam II	44
Figure 41 Predicted temperature contours for Beam II	44
Figure 42 Moment curvature variation for Beam II	44
Figure 43 Load - deflection response at various time during fire exposure for Beam II	45
Figure 44 Deflection – time response comparison for Beam II	46



List of Tables:

Table 1 Hertz constants for different aggregates	25
Table 2 Degradation factors for hot rolled reinforcement with increase in temperature [25] ..	27
Table 3 Section details of beams (Espion and Halleux, [38])	33
Table 4 Comparison of computed and experimental yield moment capacity	33
Table 5 Details of beams (Srikanth et al., [39])	35
Table 6 Comparison of computed and experimental ultimate moment capacity	35
Table 7 Properties of beam specimens (Pam et al., [41])	37
Table 8 Dimensions of beams tested by Au & Bai [42]	38
Table 9 Equivalent Modulus of Elasticity for Beam I	41
Table 10 Equivalent Modulus of Elasticity for Beam II	45



Abstract

A simplified approach to evaluate the complete-load-deflection time response of Reinforced Concrete (RC) flexural members subjected to fire loads is presented in this report. The proposed approach is extendable for performance evaluation of RC structures at all three levels of complexity namely member level (e.g. beams, columns), sub assembly level (e.g. beam-column joints) and as well as the structural level. This approach involves the determination of moment-curvature characteristics for the critical sections of the fire affected structural member and performing nonlinear static analysis to determine the load-deflection response of the member exposed to fire loads.

The thermal analysis is first performed to determine the temperature distribution across the section, for a given fire duration. Temperature-dependent stress-strain curves for concrete and steel are then utilized to perform a moment-curvature analysis. The moment-curvature relationships are obtained at regular intervals of the fire exposure. These are then utilized to obtain the load-deflection plots following nonlinear static analysis (Pushover Analysis). The load-deflection plots obtained for the different exposure durations are then used to obtain the deflection-time plots for a particular load level. Moreover, one of the important issues of modeling the initial stiffness giving due consideration to stiffness degradation due to material degradation and thermal cracking has been addressed in a rational manner. The approach is straightforward and can be easily programmed in spreadsheets.

Implementation and validation of the proposed approach with various experiments available in literature has been discussed in detail in this report. The report also discusses the in-house code developed for carrying out 2D transient heat transfer analysis and obtaining moment-curvature relationships.

Keywords:

Flexural member, fire performance, nonlinear static analysis, transient thermal analysis, lumped plasticity approach, fire exposure duration.

1 Introduction

The fire safety of any structure largely depends on the combustibility and fire rating of its main structural members. In general, concrete has good fire resistance due to its non combustible nature and low thermal conductivity. It is the high temperature that degrades material properties of concrete and reinforcing steel, which leads to failure. There have been reports in past where RC structures have suffered total or partial collapse due to the effects of fire. Beitel and Iwankiw [1] conducted an international survey of various cases of multi-storey buildings which collapsed (total or partial) due to fire. They have highlighted although total number of fire events may appear low, these fire events have high consequences with respect to potential for loss of life, injuries and economic loss.



Katrantzos Sport Department Store, Athens, Greece, (1980)



Sao Paulo Power Company (CESP) Building 2, Brazil, (1987)



Textile factory, Alexandria, Egypt, (2000)



19 Storey Apartment block, St Petersburg, Russia, (2002)

Figure 1 Structural collapses due to fire [1]

Figure 1 show few cases of RC structures which collapsed due to fire alone. Katrantzos Sport Department Store, Athens, Greece (1980) was 8 storey RC building. Although fire started on 7th floor, major part of 5-8th floors had collapsed. This incident is an example of how the performance structure as a whole is entirely different from that of an individual



member. In case of 21 storey Sao Paulo Power Company Building 2, Brazil (1987) the structural core area collapsed within 2hrs of fire. Similar was the case of a 19 storey apartment block in St Petersburg, Russia (2002) which collapsed in just 1hr of fire. Apart from these there are many other examples like Linde Factory, West Germany (1971), Minin Works, Surrey, UK (1969), Library building in Linkoping, Sweden (1996) etc where fire was the cause of structural collapse.

At present, structural fire safety is an important aspect in structural design practices, in addition to strength (at ambient conditions) and serviceability limit state. Design criteria for structural fire safety have evolved based on the standard fire tests conducted over the years; are mentioned below [2,3]:

1. Load bearing capacity (L): The member should be able to resist the applied load for the required fire rating,
2. Insulation (I): Temperature of the unexposed face of the member should be low enough to prevent the ignition of material stored against the face,
3. Integrity (E): The members should be able to confine the fire and prevent spread of fire. There should be no possibility of flame being able to reach the unexposed structure though any weakness inherent in the construction itself or due to excessive deformation during fire.

Criterion 1 and 2 can be quantified numerically/analytically. However, for criterion 3, qualification through experiment is required. For insulation criterion, a transient heat transfer analysis would be sufficient to check if the temperature of unexposed surface is within permissible limits. Load bearing capacity can be computed by resorting to a more complex coupled thermo-mechanical analysis. 3D FE analysis could be performed at element level but at structural level would be very complex, time consuming and computationally costly. Hence, there is a need of practical and scientific procedures which can be used for analysing global performance in the event of fire. The proposed procedure gives a solution to the above mentioned problem.

Before explaining the proposed procedure in detail, basic steps for evaluating fire resistance are briefly explained below. Evaluation of fire resistance of structures/members involves three basic steps:

1. First step is to estimate the various possible fire scenario(s), which the structure may experience. This step involves fire dynamics simulation or using various analytical methods to estimate the temperature distribution within a compartment. The details of this step are out of scope of this report. For further reading literature could be referred [4,5].
2. Second step is to compute the thermal gradients induced in the structural members due to the fire scenario(s) computed in step 1. This step requires a transient heat transfer analysis to be carried out. Temperature dependent thermal properties of the constituting materials act as an input to this step.



3. The third step is to compute the resulting deformations and stresses because of the thermal gradients from step 2. Temperature dependent mechanical properties of both concrete and steel act as input to this step.

This proposed approach deals with step 2 and 3 mentioned above.

2 Brief Literature Review:

2.1 Concrete at Elevated Temperature

There had been extensive experimental studies over the last 5 decades to evaluate the effect of high temperature on mechanical properties of concrete. These tests are conducted in hot state i.e., specimens are heated gradually to a target temperature, allowed to attain thermally steady state and then loaded to failure at that temperature. The principle effects of increasing temperature are reported as loss of compressive strength, reduction in modulus of elasticity and cracking. It has been well established that type of concrete (Normal strength Concrete /High strength Concrete (NSC/HSC)), aggregate type (chemical composition) and sustained load (preloading) have significant effect on the degradation properties of concrete under elevated temperature [6,7,8]. It has been noted that degradation with temperature is higher in case of siliceous aggregate as compared to calcareous aggregates. Mostly the experimental studies were confined to effect of high temperature on compressive strength and modulus of elasticity of concrete. The complete stress-strain characteristic at various temperatures has also been reported by Anderberg and Thelandresson [9], Diederichs [10] and Takeuchi et al [11]. Figure 2 and Figure 3 shows the degradation of compressive strength and modulus of elasticity respectively for NSC, as a function of temperature. The scatter is attributed to different testing procedures and chemical composition of aggregates.

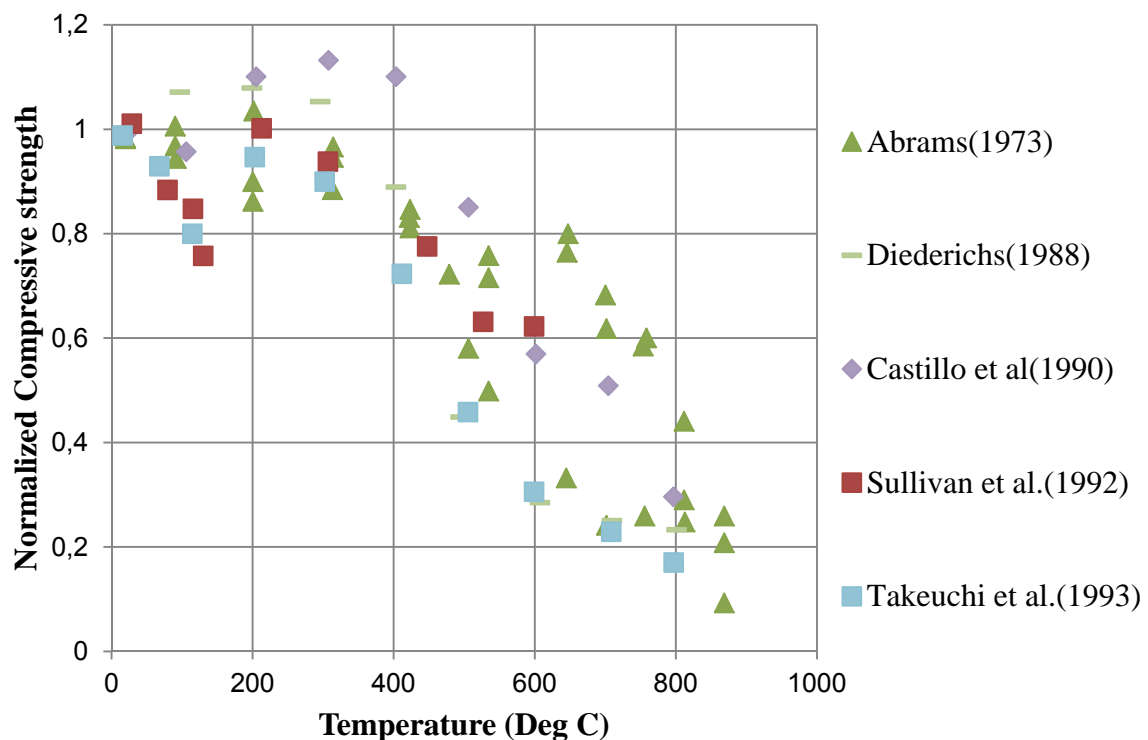


Figure 2 Variation of compressive strength of NSC with rise in temperature [6,10,12,13,11]

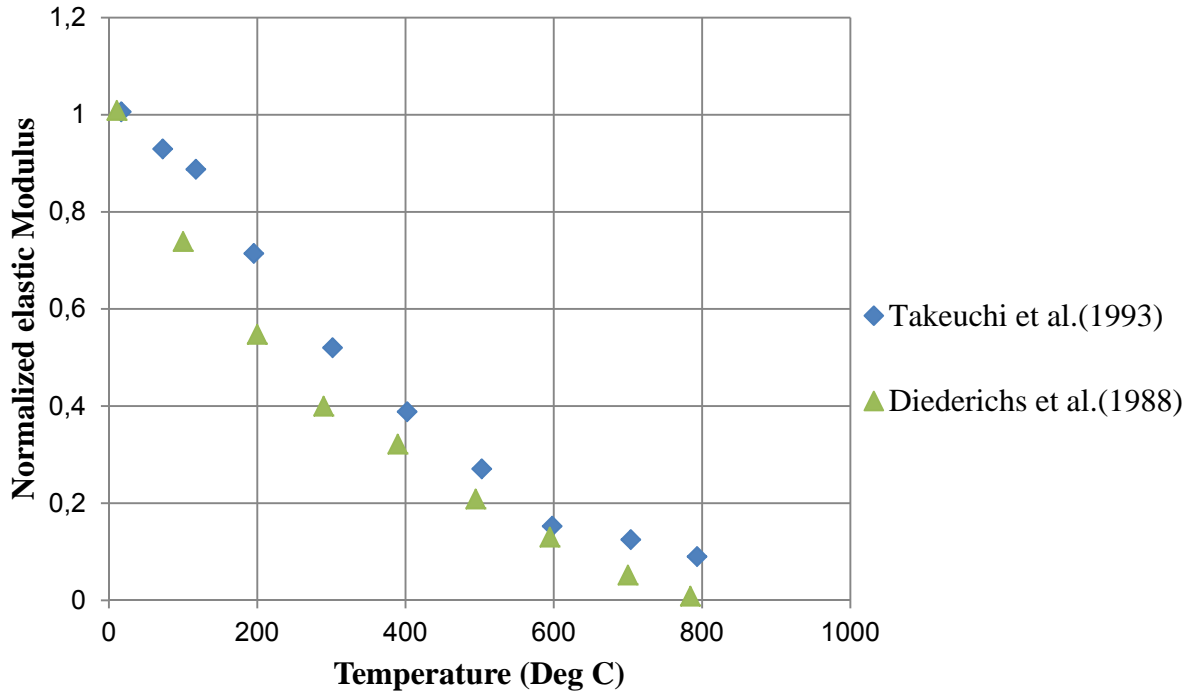


Figure 3 Variation of Modulus of Elasticity of NSC with temperature [10,11]

2.2 Experiments on RC beams under fire

The flexural capacity of RC beams, where reinforcement yielding governs the failure, is strongly influenced by the strength of reinforcing bars, while the influence of concrete compressive strength is only modest. Experimental studies on the effect of high temperature on mechanical properties of reinforcement by Takeuchi et al [11] (Ref. Figure 4) shows a steep degradation in mechanical properties above 400 °C.

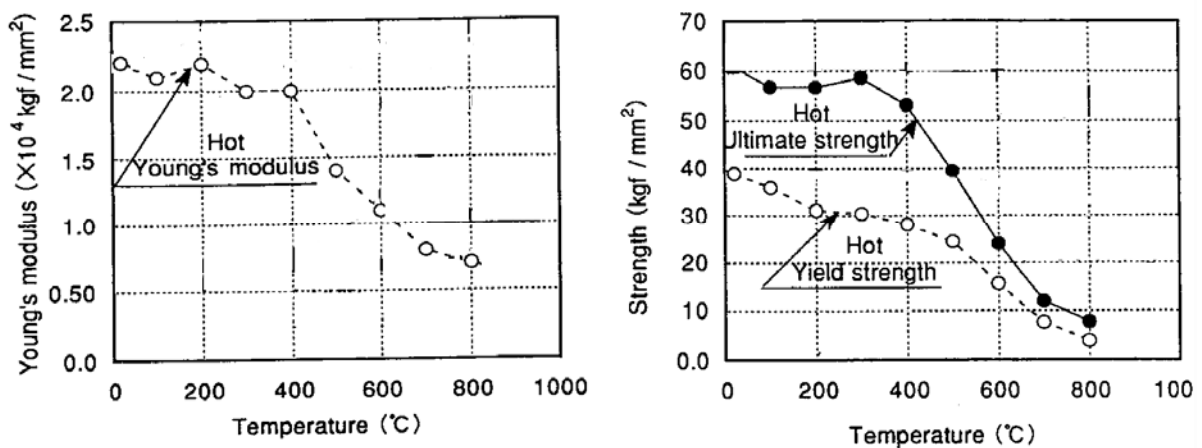


Figure 4 Variation of strength and modulus of elasticity of reinforcement bars with temperature [11]

Dotrepe [14] reported tests carried out at university of Ghent to test the fire resistance of simply supported beams. Two identical beams were tested which had a cross-section of 200 mm x 600mm and a span of 6500 mm. The beam was exposed to ISO 834 standard fire

exposure. Figure 5 shows the loading and heating system for the RC beam. Large deflections even at the beginning of the test were reported which were attributed by the author to the steep thermal gradient across the cross-section. Figure 6 shows the experimental and the numerical results of the two tested beams as reported by Dotreppe [14].

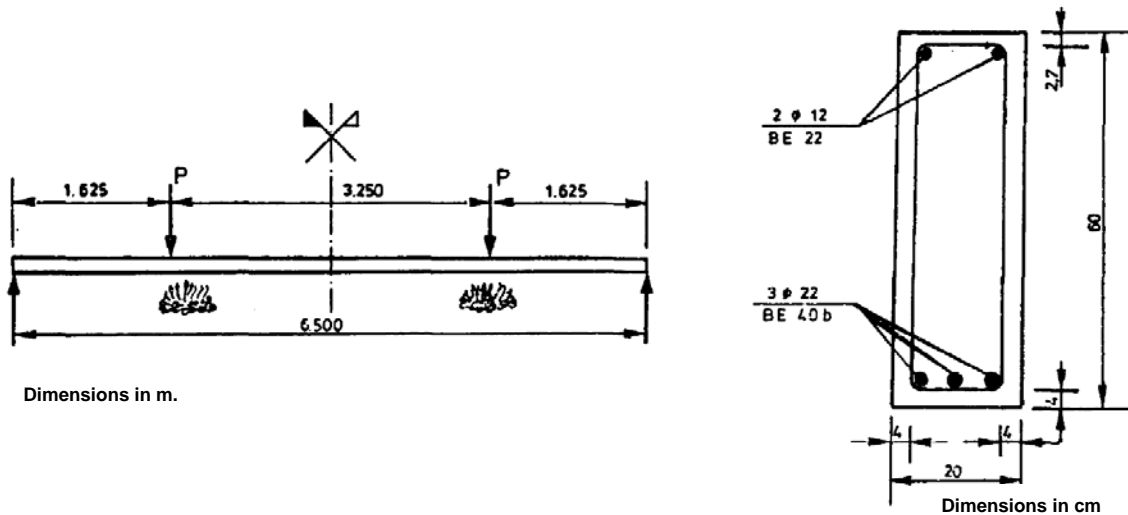


Figure 5 Loading and cross-section details of beams reported by Dotreppe [14]

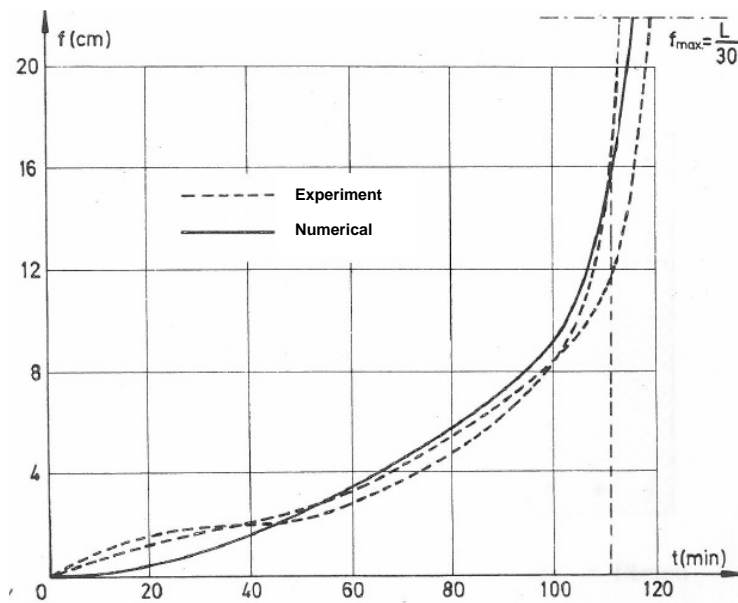


Figure 6 Experimental and numerical results of Dotreppe [14]

Lin et al. [15] tested 11 full scale RC beams under ASTM E119 standard fire exposure. The test program aimed to study/verify the effect of moment redistribution due to continuity. Hence, the test specimens were tested in such a way to represent interior span (6 specimens), end span (4 specimens) and simply supported beam (1 specimen). Various other factors investigated included type of concrete (normal weight concrete with carbonate aggregate and sanded lightweight concrete) and load level (40%, 50% and 60% of the theoretical moment capacity). The beams had a cross-section of 305 mm x 355 mm. The specimens had a span of 6100 mm between the supports and overhang of 1800 mm at both ends. Figure 7 shows the loading configuration. No spalling was observed during the fire

tests, which is attributed to using normal strength concrete. The study showed that fire endurance of continuous beams is much higher than that of simply supported beams due to redistribution of bending moment and shear force during fire. They also showed the decrease in fire endurance with increasing load level.

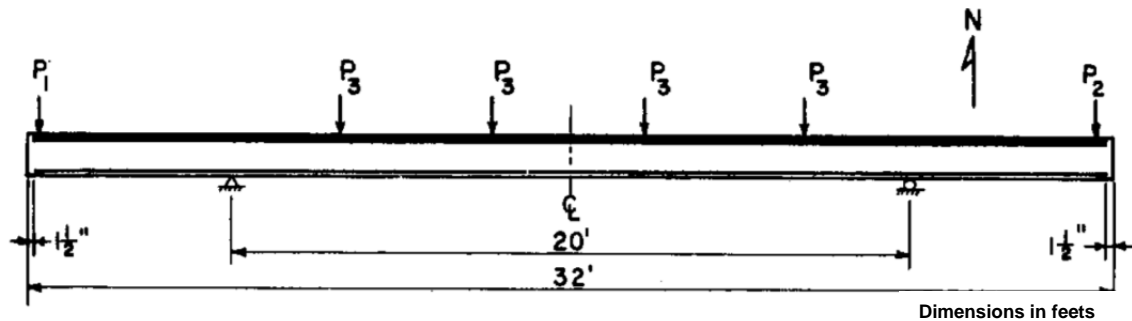


Figure 7 Loading arrangement on beams tested by Lin et al [15]

Lin et al [16] tested six full scale RC beams under large applied loads. The objective of these tests was to investigate the flexural & shear behaviour of beams and generate experimental data base for numerical validations. Five beams had the cross-section of 229 X 533 mm and one had the cross-section of 254 X 610 mm. All the beams had a total length of 8.2 m which includes 1.8 m long unexposed overhang at one end. The exposed length of beam was 6.1 m. The overhang was loaded (Ref. Figure 8) so as to provide continuity over one support. Out of 6 beams, 4 were tested under ASTM E119 standard fire and 2 were tested under a design fire which was called by authors as Short Duration High Intensity (SDHI) fire (Ref. Figure 8). During the tests the beams were loaded to produce 59% of nominal negative moment capacity at the continuous support.

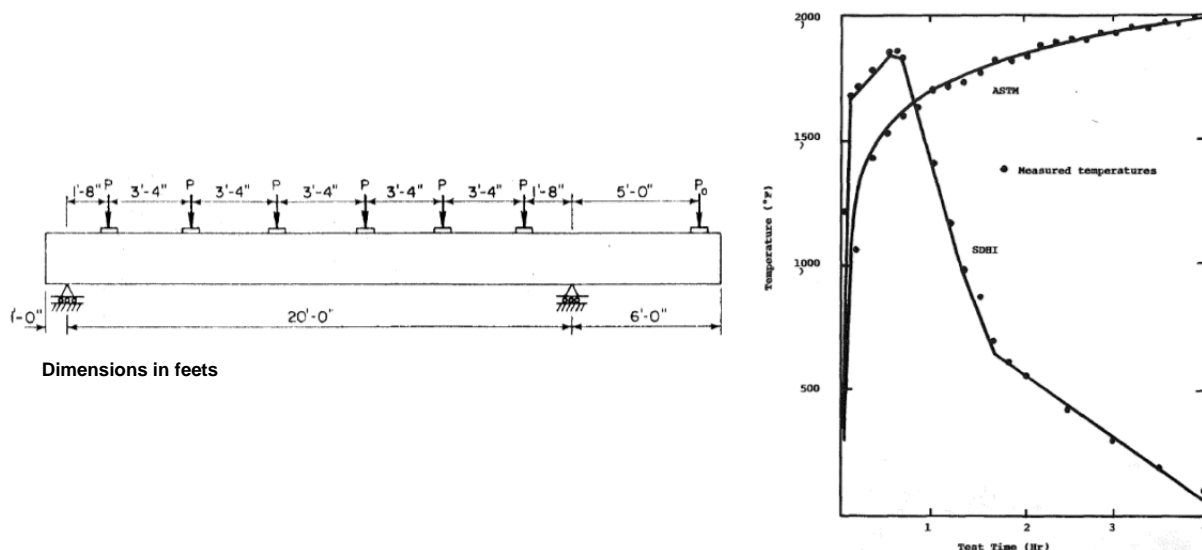


Figure 8 Load distribution and exposure on beams tested by Lin et al [16]

In all tests, first the diagonal shear cracks developed near the continuous support and then the flexural cracks formed in the maximum positive moment region. But as the tests progressed the shear cracks remained unchanged but the flexural cracks widened and propagated. Ultimately all beams formed flexural failure mechanism. Representative crack pattern is shown in Figure 9.

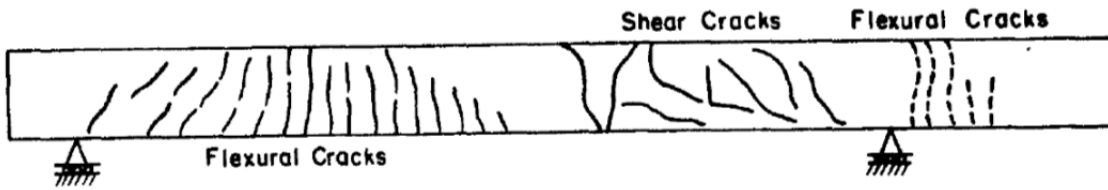


Figure 9 Crack pattern in beams tested by Lin et al [16]

Shi et al., [17] conducted tests on 13 small scale beams to study the effect of force – temperature paths on the behaviour of reinforced concrete flexural members. These paths were expressed using two basic paths: the path of constant force but subjected to elevated temperature (FT path) and the path of constant temperature but subjected to increasing forces (TF path). The beam specimens were 100 mm x 180 mm x 1300 mm, with a concrete cover of 10 mm. Beam was reinforced with 2 – 10dia low carbon plain steel bars in tension and compression. Figure 10 summarizes the test results in terms of loading ratio and temperature. (α_{FT} = ratio of ultimate bending moment resistance for FT path corresponding to temperature T_u to M_u ; α_{TF} = ratio of ultimate bending moment resistance for TF path corresponding to temperature T_o to M_u). They concluded that the fire resistance of reinforced concrete flexural members depends on the force-temperature paths acting on them.

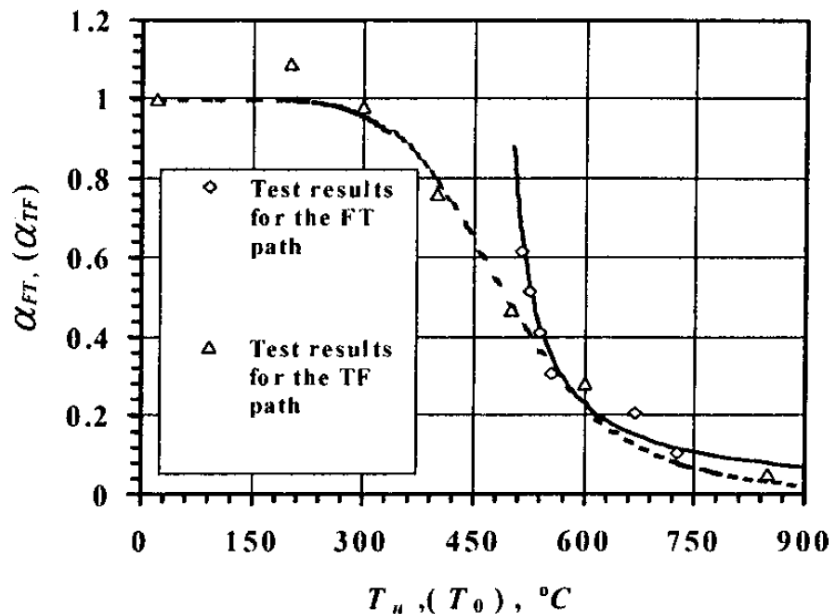


Figure 10 Fire resistance comparison for FT and TF paths [17]

Shi et al., [18] experimentally studied the influence of concrete cover (lateral and bottom) on fire resistance of RC beams. The test matrix included 6 beam specimens similar to those used for studying the effect of force-temperature paths. The depth of the beam was varied to keep the effective depth constant although the covers were different. During heating, the beams were loaded to 50% of their load carrying capacity at ambient conditions. Figure 11 shows the details of the specimen used and time-temperature variation achieved during testing. The tension reinforcement was 0.95%. The concrete cover was varied from 10 mm to 30 mm. The results conclude that concrete cover has significant influence but the influence

reduces with increasing cover thickness. Hence, it is not practical to excessively increase the bottom cover thickness to improve behaviour of RC flexural members under fire conditions.

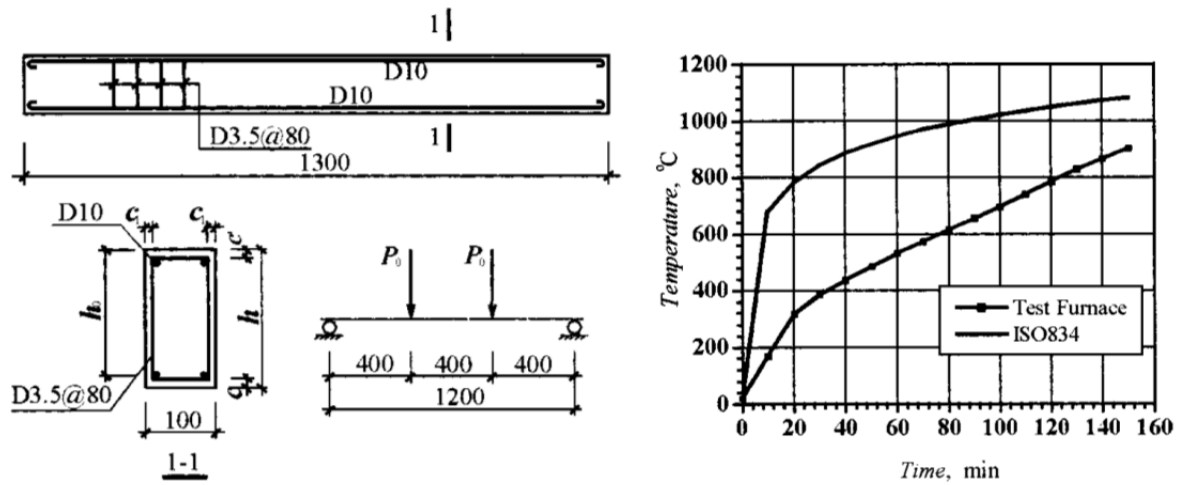


Figure 11 Specimen details and variation of furnace temperature for Shi et al. [18]

Dwaikat and Kodur [19] tested 6 full scale RC beams under ASTM E119 standard fire and two design fire scenario. Parameters investigated include concrete strength, support condition, fire scenario and load ratio. Two beams were made of Normal Strength Concrete (NSC; 52.2 MPa) and four beams were made of High Strength Concrete (HSC; 93.3 MPa). Beams were tested under simply supported condition and with axial restrains.

Dimensions of the beams were 406 x 254 x 3960 mm. Tension reinforcement consisted of 3 – 19 dia rebars and the compression reinforcement was 2 -13 dia rebars. Beams had a constant load during fire exposure, which were 55% and 65% of their ambient capacity. Figure 12 shows the deflection time responses for all the 6 beams tested. They highlighted significant difference in behaviour of beams made from HSC and NSC. The fire resistance of HSC beams is lower than that of NSC beams. This difference in behaviour is attributed to higher spalling in HSC beams (See Figure 13). Lower load level leads to higher fire resistance and also axially restrained beams have higher fire resistance.

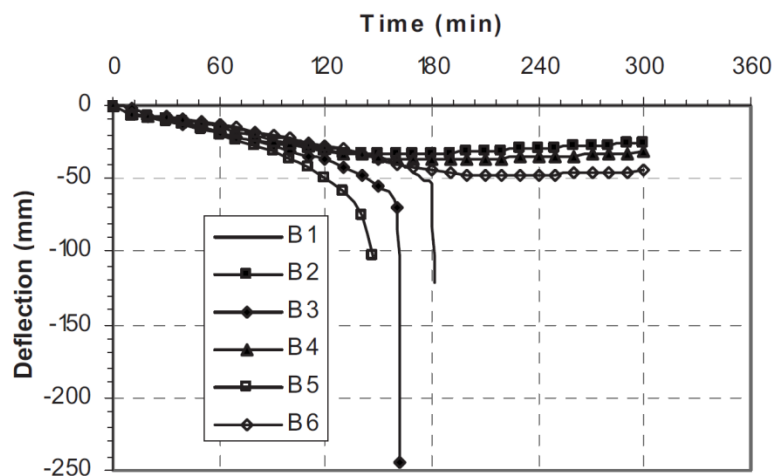


Figure 12 Deflection-time for beams tested by Dwaikat and Kodur [19]



Figure 13 Spalling in NSC and HSC beams under design fire exposure [19]

Choi and Shin [20] did an experimental study to study the effect of concrete strength and cover on the structural behavior of RC beams during fire. Two beams made of NSC (21MPa) and HSC (55 MPa) each were tested under standard ISO 834 fire scenario, until failure. The beams had total length of 4700 mm with a cross section of 250 x 400mm. Tension zone was provided with 3 – 22dia rebars and compression zone had 2 – 22dia rebars. Concrete cover was varied as 40 mm and 50 mm. The beams had a sustained load which was 55% of their ambient load carrying capacity. Figure 14 shows the deflection time graph for all the 4 beams tested. Significant spalling was observed in beams made of HSC (Ref. Figure 15). The effect of concrete cover on the fire resistance of beams made of NSC was significant but no effect was found on HSC beams mainly because of significant amount of spalling.

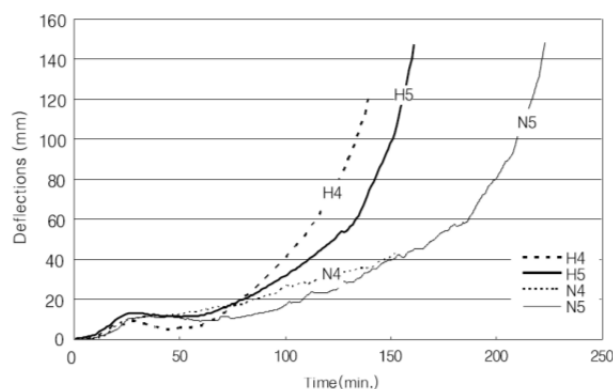


Figure 14 Deflection time for beams tested by Choi and Shin [20]



Figure 15 NSC and HSC beams at failure [20]



General conclusions based on the experimental studies discussed above are as mentioned below:

1. Fire endurance of RC beam is influenced by the concrete strength, applied load ratio, support condition, fire scenario and concrete cover.
2. The effect of concrete cover on the fire resistance of beams made of NSC was significant but increase in fire resistance is not linearly associated with cover. For beams made with HSC no significant effect of increase in cover is observed mainly because of significant amount of spalling.
3. Continuous beams exhibit higher fire endurance compared to simply-supported beams due to the possibility of moment redistribution.
4. Higher applied load ratio reduces the fire endurance.
5. NSC beams have higher fire endurance as compared to HSC mainly due to the spalling phenomenon associated with the later.
6. For shear critical beams, although diagonal shear cracks developed before the flexural cracks, the beam ultimately failed in flexure.
7. The response of RC beams during fire also depends on the fire scenario. For a design fire exposure with a cooling phase, the beam deformations continue to increase for some time even during the cooling phase. Hence, there are possibility that the beam fails during the cooling phase depending on the severity of the fire scenario.



3 Proposed approach:

Over the past few decades, efforts have been made to develop a rational methodology/procedure for evaluating the behaviour of RC flexural members during fire [21]. However, most of the proposed approaches gave empirical relations that dealt only with the strength/capacity criterion. The approach presented in this report is developed to estimate not only the load carrying capacity but also the complete load-deflection characteristics of the member.

The approach was initially developed to obtain the performance of the RC flexural members in residual state after exposure to fire [22]. This methodology basically revolves around sequential thermal-stress analysis. The cross section of the RC member is divided into $m \times n$ segments along its width and depth for analysis. Using lumped system concept, which is common approximation in transient conduction problems [23], each segment is considered to have a uniform temperature and properties (both thermal and mechanical), lumped at the center of that segment. All computations are done at the centre of the sector, which represent the complete sector. Thermal analysis is performed to determine the temperature distribution across the section, for a given fire scenario. The mechanical properties of concrete and steel in each sector are modified in accordance with the maximum temperature attained. The moment-curvature relationships are obtained for the section at regular time intervals during fire scenario. These moment-curvature characteristics were then utilized to define zero length springs that were used to obtain the load-deflection plots following nonlinear static analysis. One of the major issues in defining the spring characteristics was the definition of initial stiffness for the fire affected beams. In this work a rational approach, accounting for stiffness degradation due to material degradation and thermal cracking has been proposed. The approach is straight forward and can be easily programmed for instance in spreadsheets and can be used in conjunction with commercial software.

The proposed approach consists of following three steps:

1. Thermal Analysis: Estimation of the spatial and temporal distribution of temperature across the cross-section of the members for the given fire exposure.
2. Moment Curvature Analysis: Computation of the moment-curvature relationships for the cross-section with the temperature distribution estimated in step 1, using temperature dependent constitutive law for concrete and reinforcing bars.
3. Nonlinear Static Analysis: Performing nonlinear static analysis to obtain the complete load-deformation behaviour of the member.

The above mentioned steps are elaborated in following sections:

3.1 Basic assumption:

1. Bernoulli's Principle: Plane sections before bending remain plain after bending. This implies that longitudinal strain in the concrete and the steel at various points across a section is proportional to the distance from the neutral axis. This assumption is



reasonably accurate in the compression zone of concrete. A crack in tension implies some bond slip has occurred. However, Bernoulli's Principle holds reasonably well when applied over average tensile strain over a certain gauge length [24]. This assumption has been assumed only for mechanical strain component rather than total strain which include thermal strain and transient creep strain.

2. Tensile strength of concrete is negligible. This assumption is widely acceptable at ambient condition and is even more reasonable under fire/elevated temperature scenarios. Since, fire/elevated temperature is known to have degrading effect on mechanical properties of concrete. As per Eurocode2 [25] concrete completely loses its tensile strength at 600 °C. Also, tension zone of flexural member is directly exposed to fire.
3. No bond slip is assumed at the interface between concrete and reinforcing steel.
4. Heat transfer is considered to be 2D i.e; heat flow along the member length is neglected.
5. Thermal spalling is neglected. This assumption is acceptable in case of normal strength concrete because of its high porosity as compared to high strength concrete. Experimental observations of tests performed by Dwaikat & Kodur [19] and Choi & Shin [20], also support this assumption (Ref. Figure 13 & Figure 15).
6. Stress-strain relationship as a function of temperature for concrete as suggested by Youssef and Mofteh [26] is used.
7. Stress strain relationships as function of temperature for rebar are taken from Eurocode2 [25].
8. Thermal properties suggested by Eurocode2 for concrete have been used. Discussion on suitability of these properties can be found in Lakhani et al [27].
9. It is assumed that the temperature of rebar is equal to temperature of concrete at that location.

3.2 Thermal Analysis

To evaluate the behaviour of RC member under fire, it is required to know the amount of heat ingressed in the member i.e, temperature distribution across the cross section should be known. Heat transfer from the surrounding hot gases to the member surface takes place by means of convection and radiation. Within the member heat is transferred through conduction. This complete process of heat transfer is transient in nature due to the variation of gas temperature with time. The governing differential equation for 2D transient heat conduction problem is given by Eq. (1). The governing equation is solved using Central Difference Method and iterative solver to obtain the spatial and temporal distribution of temperature, $T(x,t)$.



$$\rho c \frac{\partial T}{\partial t} = k \left[\frac{\partial^2 T}{\partial x^2} + \frac{\partial^2 T}{\partial y^2} \right] \quad (1)$$

The following Eq. (2) states the boundary condition that needs to be satisfied.

$$-k \frac{\partial T}{\partial n} = h[T_g - T_s] + \varepsilon \sigma [(T_g + 273)^4 - (T_s + 273)^4] \quad (2)$$

Where:

- k is the thermal conductivity (W/m °C),
- ρ is the mass density (kg/m³),
- c is the specific heat of solid (J/kg. °C),
- h is convective heat transfer coefficient (W/m² °C),
- ε is Stephen Boltzmann constant (5.667 x 10⁻⁸ W/m² °K⁴),
- σ is surface emissivity,
- T_g is gas temperature (°C),
- T_s is surface temperature (°C).

Thermal properties of concrete as function of temperature used are shown in Figure 16. These properties are taken for Eurocode2 [25].

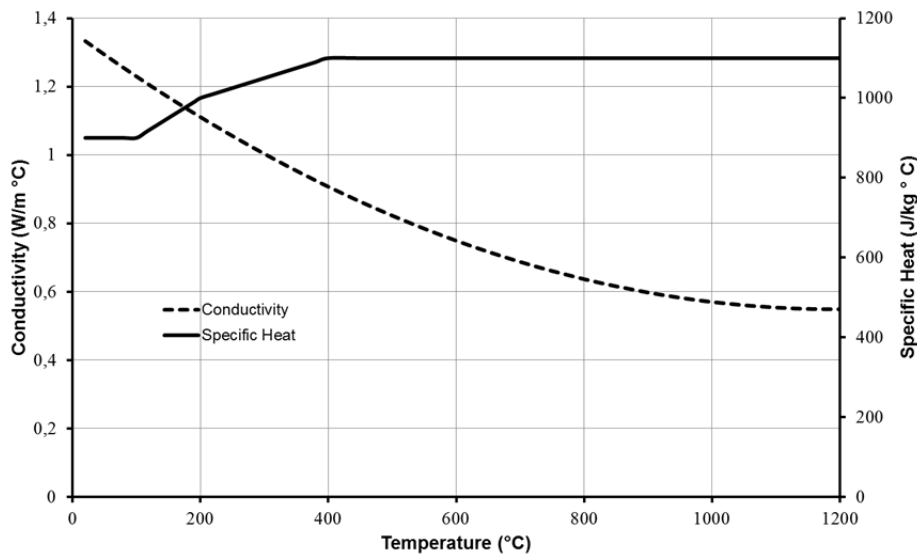


Figure 16 Thermal properties of concrete

3.3 Moment Curvature Analysis

The load-deflection characteristics of RC flexural members are mainly dependent on the moment curvature characteristics of the section [24]. Moment curvature relationships for RC sections are derived based on assumptions similar to those of theory of simple bending (Ref section on Basic Assumptions). For determining the moment curvature relation, stress strain relationships for concrete and reinforcing bars are required. In the present case, these stress strain relations are required as functions of temperature.

3.3.1 Temperature dependent Stress – Strain relationship for Concrete

Various researchers have suggested constitutive laws of varying simplicity for unconfined as well as confined concrete at ambient temperature [28,29,30]. Out of these, the stress strain curve for concrete confined by rectangular stirrups as suggested by Kent and Park [28] has been shown to provide results in excellent correspondence with experiments [31]. Furthermore, the model offers a good balance between simplicity of application and accuracy of results. For concrete at elevated temperatures, the strength reduction as a function of temperature for unconfined concrete has been reported by various researchers. These studies have been well reviewed and compared by Li & Purkiss [32] and Youssef & Mofteh [26]. Youssef and Mofteh [26] extended the model by Scott et al. [33] (Modified Kent and Park [28] model) to define the stress-strain curve for confined concrete at elevated temperature. In this work, a similar model has been employed as the constitutive law for concrete in compression. Equations (3) to (7) defines the curve shown in Figure 17 mathematically. For the model used, f'_{cT} and ε_{oTc} were calculated using the formulation Eqn. (8) & (9) proposed by Hertz [34] and Terro [35] respectively.

$$f_{cT} = f'_{cT} \left[2.0 \left(\frac{\varepsilon_{cT}}{\varepsilon_{oTc}} \right) - \left(\frac{\varepsilon_{cT}}{\varepsilon_{oTc}} \right)^2 \right] \quad \varepsilon_{cT} \leq \varepsilon_{oTc} \quad (3)$$

$$f_{cT} = f'_{cT} [1 - Z(\varepsilon_{cT} - \varepsilon_{oTc})] \geq 0.2f'_{cT} \quad \varepsilon_{cT} \geq \varepsilon_{oTc} \quad (4)$$

$$Z = \frac{0.5}{\varepsilon_{50uT} + \varepsilon_{50h} - \varepsilon_{oTc}} \quad (5)$$

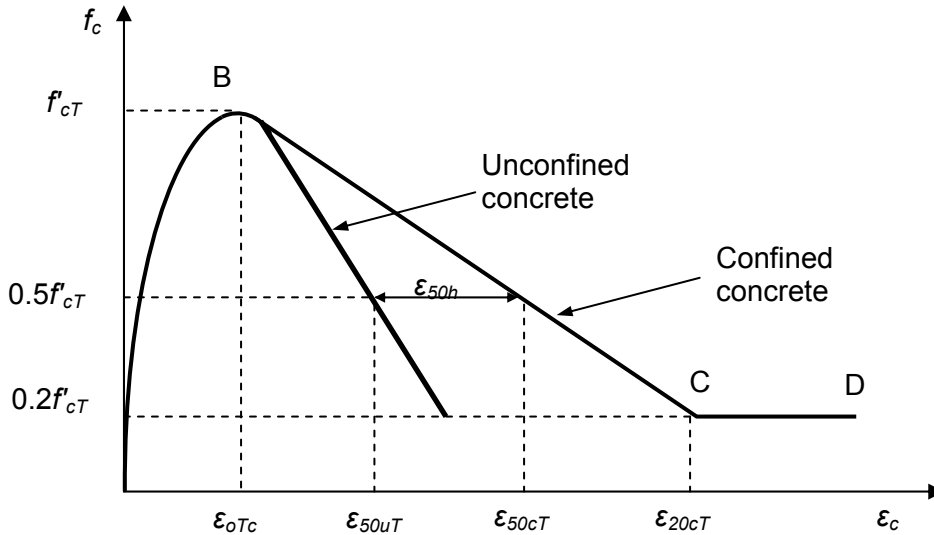


Figure 17 Temperature dependent stress strain curve for concrete in compression [26]

$$\varepsilon_{50uT} = \frac{3 + 0.29f'_{cT}}{145f'_{cT} - 1000} \cdot \frac{\varepsilon_{oTc}}{\varepsilon_{oc}} \quad (6)$$

$$\varepsilon_{50h} = 0.75\rho_s \sqrt{\frac{h'}{s_h}} \quad (7)$$



$$f'_{cT} = f'_c \cdot \left[\frac{1}{1 + \frac{T}{T_1} + \left(\frac{T}{T_2}\right)^2 + \left(\frac{T}{T_8}\right)^8 + \left(\frac{T}{T_{64}}\right)^{64}} \right] \quad (8)$$

$$\varepsilon_{oTc} = (50\lambda_L^2 - 15\lambda_L + 1) \cdot \varepsilon_{o1} + 20 \cdot (\lambda_L - 5\lambda_L^2) \cdot \varepsilon_{o2} + 5 \cdot (10\lambda_L^2 - \lambda_L) \cdot \varepsilon_{o3} \quad (9)$$

$$\varepsilon_{o1} = 2.05 \times 10^{-3} + 3.08 \times 10^{-6} \cdot T + 6.17 \times 10^{-9} \cdot T^2 + 6.58 \times 10^{-12} \cdot T^3 \quad (10)$$

$$\varepsilon_{o2} = 2.03 \times 10^{-3} + 1.27 \times 10^{-6} \cdot T + 2.17 \times 10^{-9} \cdot T^2 + 1.64 \times 10^{-12} \cdot T^3 \quad (11)$$

$$\varepsilon_{o3} = 0.002 \quad (12)$$

Where:

f_{cT}	Concrete compressive stress at temperature 'T'
f'_{cT}	Concrete compressive strength at temperature 'T'
ε_{cT}	Concrete strain at temperature 'T'
ε_{oTc}	Strain corresponding to maximum stress at temperature 'T'
Z	Slope of the descending branch of the concrete stress-strain curve
ε_{50uT}	Strain corresponding to 50% the peak stress, on the descending branch of stress-strain curve of unconfined concrete at temperature 'T'
ε_{oc}	Strain at maximum stress at ambient conditions
ε_{50h}	Additional strain component due to confinement
ρ_s	Ratio of volumn of transverse reinforcement to the volumn of the concrete core measured to outside the transverse reinforcement
h'	Width of concrete core measure to outside of the transverse reinforcement
S_h	Centre to centre spacing of the transverse reinforcement
T	Temperature
λ_L	Factor accounting for initial compressive stress level, Terro [35]
T_1, T_2, T_8, T_{64}	Constants describing the reduction in the concrete compressive strength for different aggregate type, Hertz [34] (Ref. Table 1)

Table 1 Hertz constants for different aggregates

Constant	T_1	T_2	T_8	T_{64}
Siliceous aggregate	15,000	800	570	100,000
Lightweight aggregate	100,000	1,100	800	940
Other aggregates	100,000	1080	690	1000

3.3.2 Temperature Dependent Stress – Strain relationship for Reinforcement

Stress strain relationship for reinforcing steel shown in Figure 18 was used, as suggested by Eurocode2 [25], at elevated temperature. Table 2 gives the variation of salient points on stress strain curve of hot rolled reinforcing steel with increasing temperature. Important characteristics regarding mechanical properties of reinforcing bars at elevated temperature are: with increase in temperature yield strength decreases significantly after 500 °C; although yield strength is almost intact below 400 °C but the proportional limit and elastic modulus decreases significantly. In other words the assending branch of the stress strain curve becomes more non-linear (Ref. Figure 18). This increase in nonlinearity would result in higher plastic rotation during fire. Equation (13) to (20) gives the mathematical formulation of

the stress strain curve as per Eurocode2. Although Eurocode2 model does not have hardening but in present model hardening has also been considered. It is assumed that the degradation factors for the yield strength are also applicable to ultimate strength.

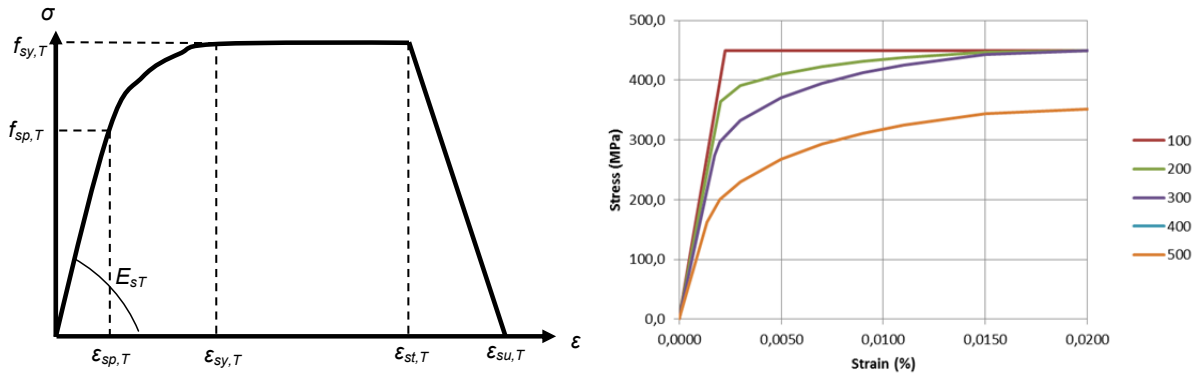


Figure 18 Stress strain curve for reinforcing steel

$$f_{sT} = \varepsilon E_{s,T} \quad \varepsilon < \varepsilon_{sp,T} \quad (13)$$

$$f_{sT} = f_{sp,T} - c + (b/a)[a^2 - (\varepsilon_{sy,T} - \varepsilon)^2]^{0.5} \quad \varepsilon_{sp,T} \leq \varepsilon \leq \varepsilon_{sy,T} \quad (14)$$

$$f_{sT} = f_{sy,T} \quad \varepsilon_{sy,T} \leq \varepsilon \leq \varepsilon_{st,T} \quad (15)$$

$$f_{sT} = f_{sy,T} [1 - (\varepsilon - \varepsilon_{st,T}) / (\varepsilon_{su,T} - \varepsilon_{st,T})] \quad \varepsilon_{st,T} \leq \varepsilon \leq \varepsilon_{su,T} \quad (16)$$

$$f_{sT} = 0 \quad \varepsilon = \varepsilon_{su,T} \quad (17)$$

Where,

- E_s Slope of the linear elastic region under ambient conditions
- $E_{s,T}$ Slope of the linear elastic region at temperature 'T'
- f_{sT} Stress in reinforcing steel
- $f_{sp,T}$ Stress corresponding to proportional limit
- f_{yk} Characteristic yield stress at ambient temperature
- $f_{sy,T}$ Yield stress at temperature 'T'
- ε Strain in reinforcing steel
- $\varepsilon_{sp,T}$ Strain corresponding to the proportional limit ($=f_{sp,T}/E_{s,T}$)
- $\varepsilon_{sy,T}$ Strain corresponding to yielding ($=0.02$)
- $\varepsilon_{st,T}$ Strain marking to onset of descending branch ($=0.15$)
- $\varepsilon_{su,T}$ Ultimate strain value ($=0.20$)
- a, b, c Functions expressed as (Equation (18) to (20)):

$$a^2 = (\varepsilon_{sy,T} - \varepsilon_{sp,T})(\varepsilon_{sy,T} - \varepsilon_{sp,T} + c/E_{s,T}) \quad (18)$$

$$b^2 = c(\varepsilon_{sy,T} - \varepsilon_{sp,T})E_{s,T} + c^2 \quad (19)$$

$$c = \frac{(f_{sy,T} - f_{sp,T})^2}{(\varepsilon_{sy,T} - \varepsilon_{sp,T})E_{s,T} - 2(f_{sy,T} - f_{sp,T})} \quad (20)$$



Table 2 Degradation factors for hot rolled reinforcement with increase in temperature [25]

Temp	Yield Strength	Youngs Modulus	Proportional Limit
°C	$f_{sy,T}/f_{yk}$	$f_{sp,T}/f_{yk}$	$E_{s,T}/E_s$
20	1.00	1.00	1.00
100	1.00	1.00	1.00
200	1.00	0.90	0.81
300	1.00	0.80	0.61
400	1.00	0.70	0.42
500	0.78	0.60	0.36
600	0.47	0.31	0.18
700	0.23	0.13	0.07
800	0.11	0.09	0.05
900	0.06	0.07	0.04
1000	0.04	0.04	0.02
1100	0.02	0.02	0.01

3.3.3 Generation of moment-curvature characteristics

The complete procedure for calculating Moment-Curvature relationship is explained with a flow chart shown in Figure 19. For further details of the theory, Park and Paulay [24] may be referred.

The symbols used in Figure 19 are described below:

$A_{R,k}$	Area of k^{th} reinforcement bar (mm^2)
A_{sec}	Area of sector (mm^2)
B	Width of the beam (mm)
D	Total depth of the beam (mm)
d'	Clear cover (mm)
$d_{R,k}$	Diameter of k^{th} reinforcement bar (mm)
$F_{\text{comp,c}}$	Total compressive force in concrete (N)
$F_{\text{comp,R}}$	Total compressive force in reinforcement bars (N)
$F_{\text{Ten,R}}$	Total tensile force in reinforcement bars (N)
i, j	Integers for identification of sector (Nos.)
k	Integer for identification of reinforcement bar (Nos.)
m	Number of sectors in X-Direction (along width) (Nos.)
M	Moment of resistance of the section at curvature ϕ (N-mm)
n	Number of sectors in Y-Direction (along depth) (Nos.)
N_R	Total number of longitudinal reinforcement bars in beam (Nos.)
$T_{i,j}$	Temperature of sector (i,j) (deg C)
$tol.$	Tolerance (convergence criterion)
$T_{R,k}$	Temperature of k^{th} reinforcement bar (deg C)
$X_{R,k}$	Horizontal distance to the centre of k^{th} rebar for bottom left corner of section (mm)
X_u	Depth of neutral axis from extreme compression fiber of the section (mm)
$Y_{R,k}$	Vertical distance to the centre of k^{th} rebar for bottom left corner of section (mm)



$\varepsilon_{c,ij}$	Strain in concrete of sector (i,j) (Unitless)
$\varepsilon_{c,ult}$	Ultimate strain in concrete (from constitutive law) (Unitless)
$\varepsilon_{R,k}$	Strain in k^{th} reinforcement bar (Unitless)
$\varepsilon_{R,ult}$	Ultimate strain in reinforcement (from constitutive law) (Unitless)
ε_u	Strain at extreme compression fiber of the section (Unitless)
ϕ	Curvature of beam (rad/mm)
$\sigma_{cT,ij}$	Stress in concrete of sector (i,j) at temperature T (MPa)
$\sigma_{RT,k}$	Stress in k^{th} reinforcement bar at temperature T (MPa)

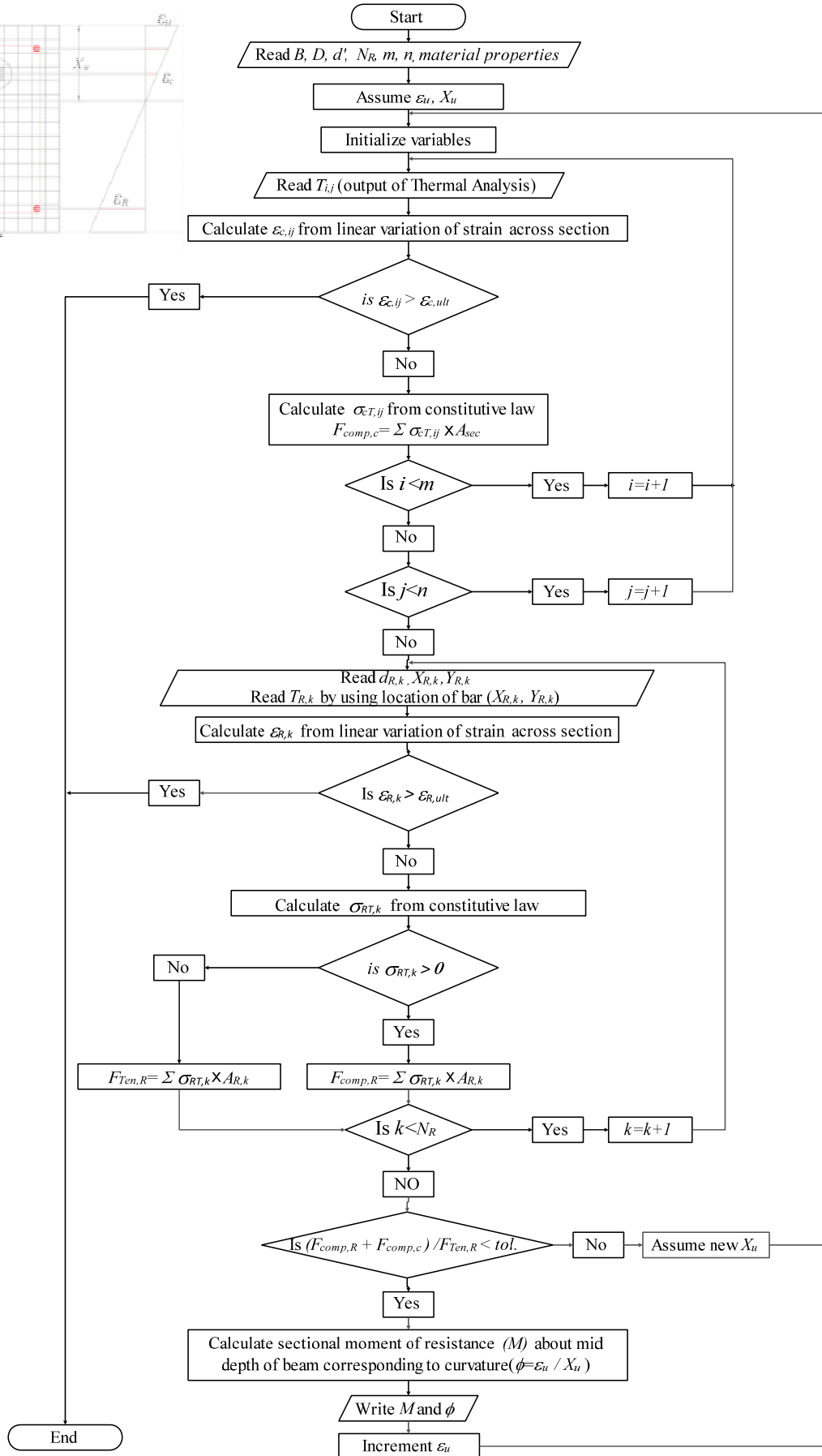
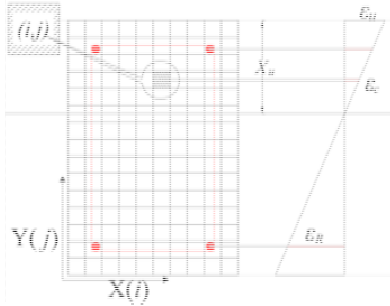


Figure 19 Flowchart for moment-curvature analysis



3.4 Nonlinear Static Analysis

The modelling was performed within the framework of stiffness matrix analysis and lumped plasticity approach using commercial software SAP2000®. The beam was modelled using 3D beam element with six degrees of freedom at each node. The hinge characteristics, once obtained, were assigned to the beam model at critical locations. The hinge is basically a zero length rotational spring with non linear characteristics defined by the moment-rotation relationship. The computing the moment-rotation characteristics from moment-curvature characteristics, plastic hinge length (l_p) is taken as half the effective depth (d) of the section ($l_p=0.5 \times d$).

One of the major issues in defining the spring characteristics is the definition of initial modulus of elasticity for the fire affected beams. The initial uncracked modulus of elasticity, E_c , (ambient conditions) is considered as $4730(f_c)^{0.5}$ [36]. First cracking is not modelled explicitly, its effect is accounted for by taking cracked modulus of elasticity (E_{cr}) as half the value for uncracked modulus of elasticity as recommended by FEMA 440 [37].

The stiffness of the fire affected RC structural member is much lesser compared to that of the RC beams tested at ambient temperature. The reason for that is two-fold: (i) degradation in modulus of elasticity of materials (concrete and steel) with rise in temperature and (ii) when the beams are subjected to fire, cracks are induced due to thermal gradients. Thus, the modulus of elasticity to be used in the analysis of a beam during fire is proposed as:

$$E_{ct} = k_1 k_2 E_{cr} \quad (21)$$

Where,

- E_{ct} is the effective modulus of elasticity for sections exposed to fire of duration 't' hrs
 t is the duration of fire exposure (heating phase only)
 E_{cr} is the modulus of elasticity for cracked concrete given as $0.5 \times 4730(f_c)^{0.5}$ (ACI 318, 2011)
 k_1 is the factor to account for reduction in stiffness due to material degradation
 k_2 is the factor to account for thermal cracking

The procedure for computing factor k_1 for reduction in stiffness of the fire affected beams due to material degradation involves following steps:

1. The moment-curvature characteristic for the section at ambient temperature and at regular time intervals during the fire exposure was evaluated.
2. The slopes (k_ϕ) of the initial (linear) portion of moment-curvature relationships for all moment-curvature relationships obtained in step 1 were evaluated.
3. The computed k_ϕ for fire affected beams are then normalized with respect to that of ambient temperature. The plot of normalized k_ϕ with fire exposure duration gives us k_1 factor. The normalized k_ϕ value obtained by the fitted equation is considered as k_1 .



The value of k_2 factor would depend on severity of exposure, duration of exposure, loading state of the member etc because these factors would in turn affect the cracking induced in the member. In order to maintain the simplicity and ease of applicability of this method a value of 0.4 for k_2 factor based on the validations shown in further sections, is proposed.



4 Validation against experiments

The approach described above has been implemented using Visual Basic (VB) macros in MSExcel[®]. The program is capable of performing 1D (as for slab and walls) and 2D (as for beams) transient heat transfer analysis, plotting temperature contours and computing temperature dependent moment curvature relationship for the given section under standard fire or user defined fire scenarios. It also gives user the flexibility to define concrete strength degradation as a function of aggregate type. User defined degradations of various mechanical properties for reinforcement can also be defined.

This section of the report provides the validation of the proposed approach and the implementation done. The validation is presented both at ambient conditions and during fire cases.

4.1 Moment Curvature at Ambient Temperature

4.1.1 Espion and Halleux [38]

They tested 12 rectangular reinforced concrete beams under bending and constant axial force. The parameters investigated were intensity of axial force and amount of reinforcement. The axial load was varied from 0 kN to 300 kN. The beams tested without axial force are reported here. Table 3 lists the reinforcement details for 3 beams used of validating the computed moment – curvature relationships. All beams had a cross section of 150 mm x 280 mm and total length of 3m. The beam was tested under four point bending with the two loads placed at 1/3rd and 2/3rd of the beam length. There was no shear reinforcement between the two loading points. The mean cylinder strength of concrete was reported as 41.6 MPa. Yield strength for reinforcing bars was 510 MPa. Experimentally the curvature was evaluated in the central section using the strains recorded along five equidistance fibers on both vertical sides: Comparison of computed moment capacity with experimental values is shown in Table 4. Figure 20 to Figure 22 shows the comparison of experimental moment curvature with the calculated moment-curvature. It may be noted that complete moment-curvature was not reported experimentally because the main objective of the experiments was to study the tension stiffening effect and its importance in verification of serviceability limit state. It can be observed that the comparison is reasonably good both in terms of capacity and moment curvature.

Table 3 Section details of beams (Espion and Halleux, [38])

Beam	A_{st}	A_{sc}	d (mm)	d' (mm)
N0-D-1.2	3-14 Φ	3-14 Φ	250.8	34
N0-D-1.4	2-18 Φ	2-18 Φ	250.2	38.9
N0-S-1.4	2-18 Φ	-	250.2	-

A_{st} = Tension reinforcement; A_{sc} = Compression reinforcement; d = distance from extreme compression fiber to centroid of tension reinforcement; d' = distance from extreme compression fiber to centroid of compression reinforcement.

Table 4 Comparison of computed and experimental yield moment capacity

Beam	Moment Capacity(kN-m)	
	Experimental [38]	Computed
N0-D-1.2	54.0	55.17



N0-D-1.4	57.0	59.80
N0-S-1.4	59.0	59.36

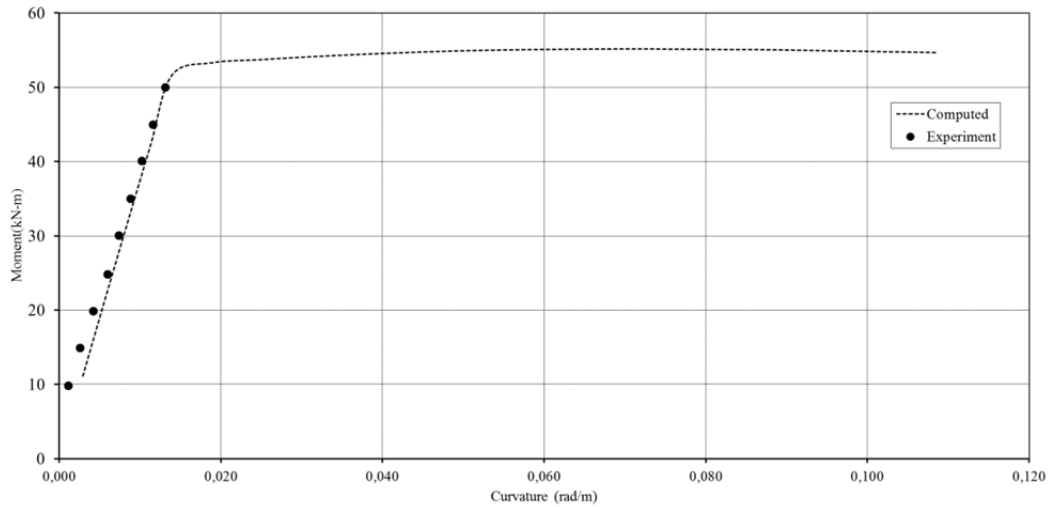


Figure 20 Computed and experimental moment - curvature for beam N0-D-1.2

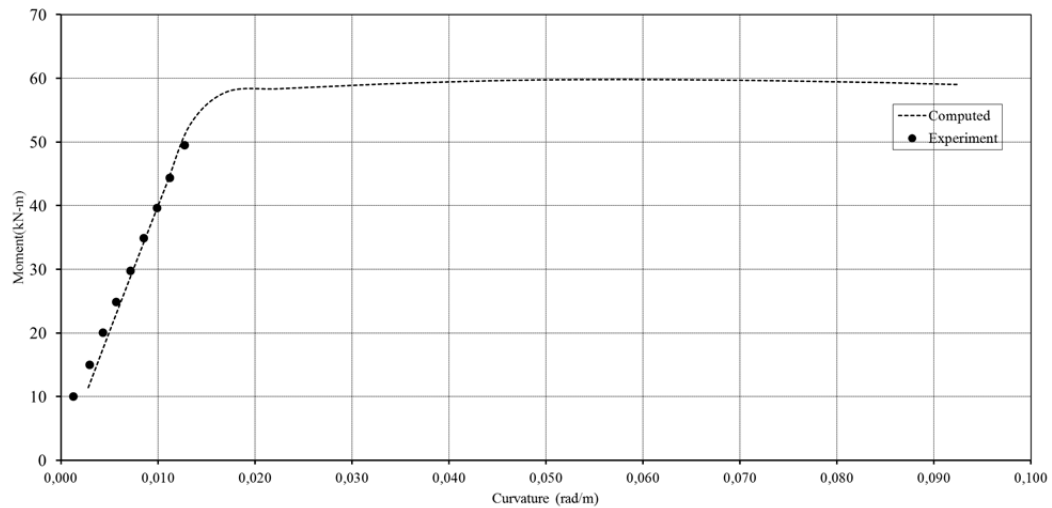


Figure 21 Computed and experimental moment - curvature for beam N0-D-1.4

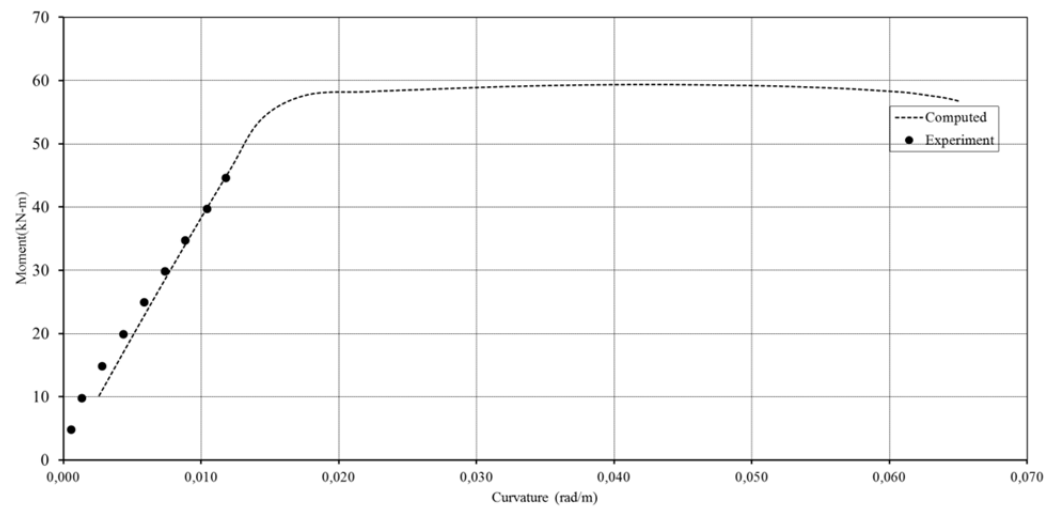


Figure 22 Computed and experimental moment - curvature for beam N0-S-1.4



4.1.2 Srikanth, Kumar and Giri [39]

A total of 6 RC beams of cross-section 150 x 200 mm and 2100 mm long were tested to obtain the moment curvature for validating the numerical procedure. Three beams from this experimental study are picked for validating the computations made. Details of the beams are given in Table 5. All beams had a shear reinforcement of 8mm stirrup @ 125 mm c/c. Gi wires of 2 – 4 mm were used as hanger bars in the compression zone. Table 6 shows that the computed ultimate moment capacity, agree well with the experimental values. Figure 23 to Figure 25 shows a good match between the computed experimental and computed moment-curvature plots. The sudden drop after the plateau region in computed moment-curvature plots is because it accounts for spalling of cover concrete in compression.

Table 5 Details of beams (Srikanth et al., [39])

Beam	f_c (MPa)	A_{st}	f_y (MPa)
U1	42.54	2-12 Φ	400.85
U2	39.65	2-16 Φ	409.55
U3	47.92	2-16 Φ	409.55

f_c = Average Cube (150 x 150 x 150mm) strength of concrete; A_{st} = Tension reinforcement; f_y = Yield strength of reinforcement.

Table 6 Comparison of computed and experimental ultimate moment capacity

Beam	Moment Capacity(kN-m)	
	Experimental [39]	Computed
U1	16.55	15.00
U2	24.29	25.00
U3	24.55	25.52

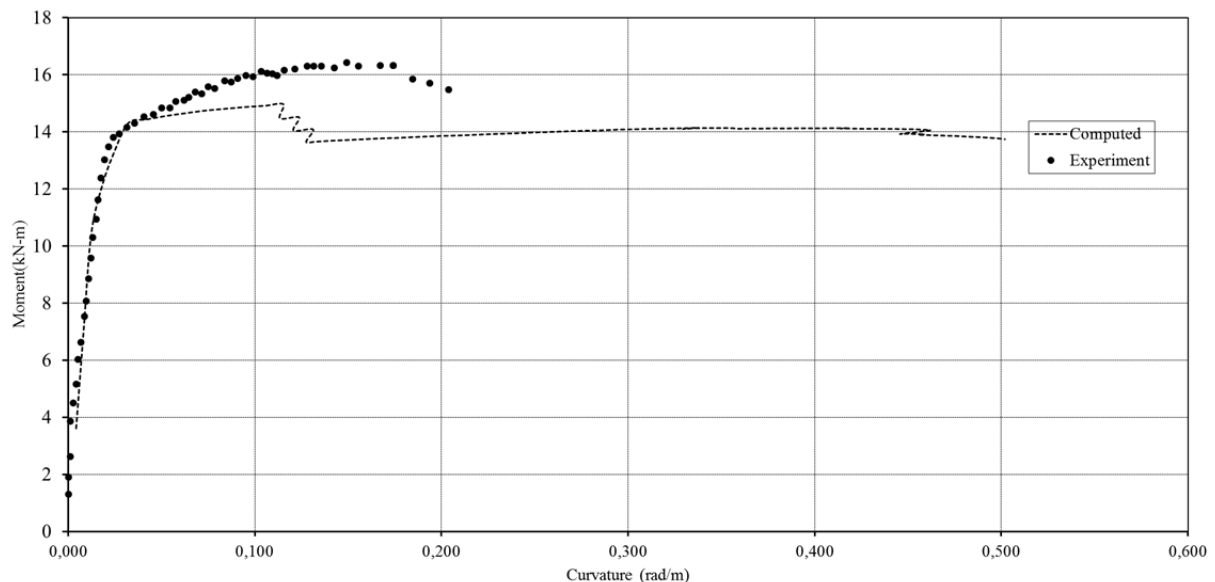


Figure 23 Computed and experimental moment - curvature for beam U1

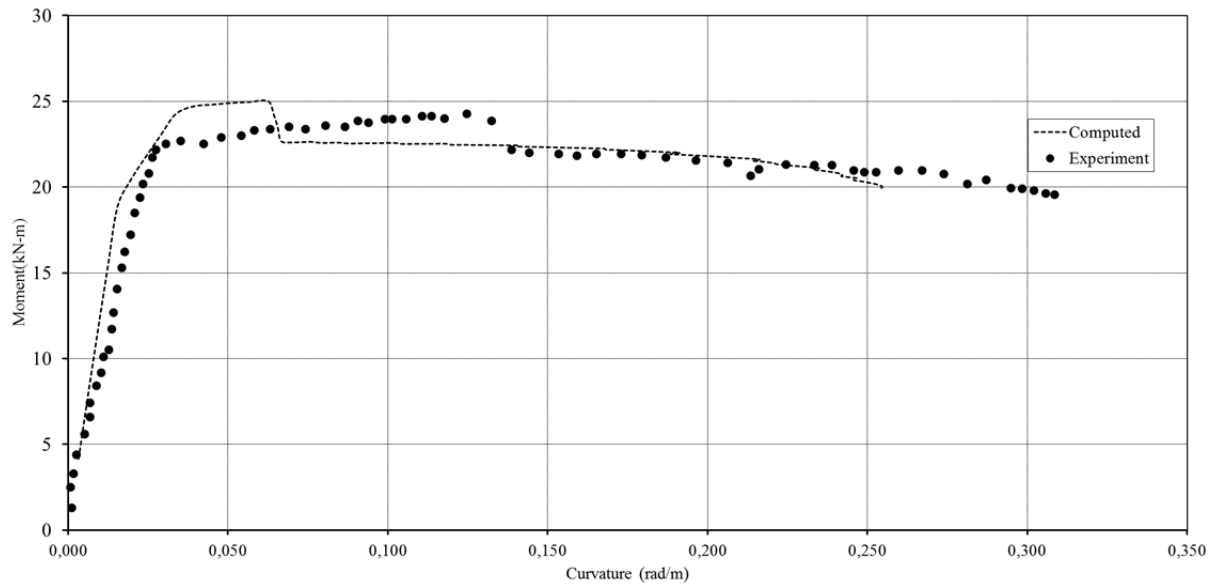


Figure 24 Computed and experimental moment - curvature for beam U2

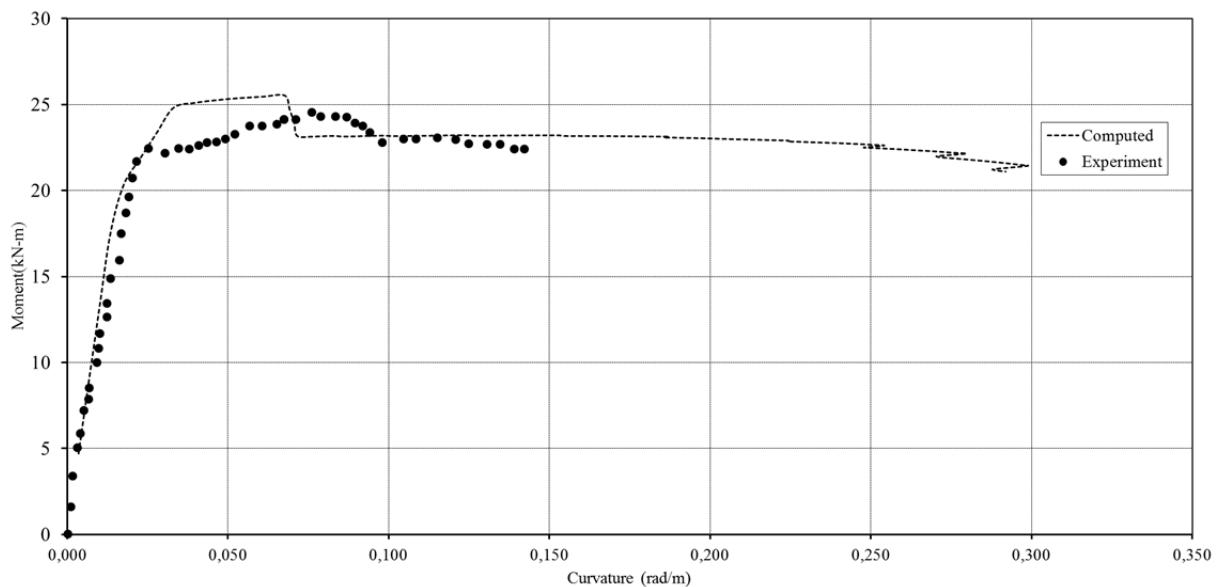


Figure 25 Computed and experimental moment - curvature for beam U3

4.2 Nonlinear Static Analysis at ambient temperature to obtain load-deflection behaviour

The inelastic analysis (non-linear static) was performed using commercial software SAP2000®. The modelling was done within the framework of stiffness matrix analysis and lumped plasticity approach. The beams were modelled using 3D beam element with six degrees of freedom at each node. The hinge characteristics, once obtained, were assigned to the beam model at critical locations. The hinge is basically a zero length rotational spring with non linear characteristics defined by the moment-rotation relationship. Plastic hinge length (l_p) was taken as half the effective depth (d) of the section ($l_p=0.5 \times d$), as recommended by Paulay & Priestley [41] for computing the moment-rotation characteristics from moment-curvature characteristics. Since, first cracking has not been modelled explicitly, cracked modulus of elasticity was used ($E_{c,cr} = 0.5 \times E_{c,uncracked}$).

4.2.1 Pam, Kwan and Islam [40]

A total of 20 singly reinforced concrete beams of 200 x 300 x 3000 mm (effective span of 2600 mm) were tested under monotonically increasing load. The parameters studied were concrete strength (35 -100 MPa) and percentage reinforcement (0.8 % to 5.5 %). The objective of these tests was to study the flexural behaviour of RC beams made from normal and high strength concrete. Two beam specimens were selected to validate the inelastic analysis procedure to obtain the load - deflection characteristics. Figure 26 shows the beam cross-section and loading arrangement used during testing. Various properties of the beam specimens are summarized in Table 7. Figure 27 show a good comparison between the experimental and computed Moment vs mid span deflection curve.

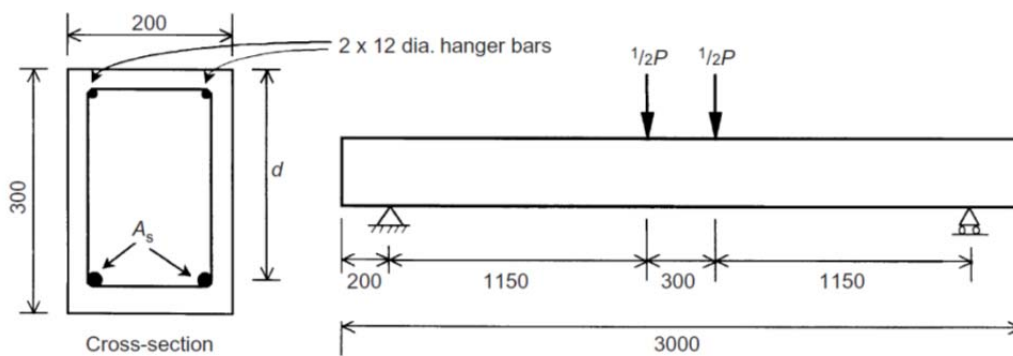


Figure 26 Cross Section details and loading arrangement (Pam et al., [41])

Table 7 Properties of beam specimens (Pam et al., [41])

Beam	f_c (MPa)	d (mm)	A_{st}	f_y (MPa)
B2	36.8	264	3-16 Φ	579
B8	57.1	260	3-25 Φ	520

f_c = Average Cube strength of concrete; A_{st} = Tension reinforcement; f_y = Yield strength of reinforcement.

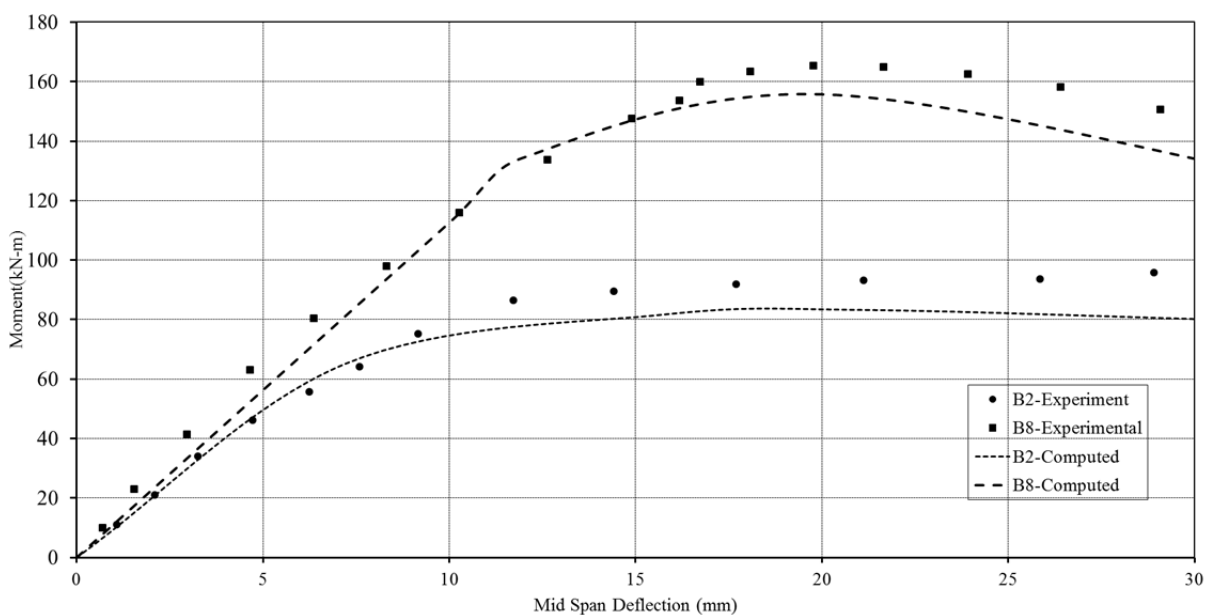


Figure 27 Computed and experimental Moment – Deflection curves for beam B2 & B8



4.2.2 Au and Bai [42]

To validate their two dimensional nonlinear finite element procedure they tested two beams under monotonic increasing loads. These two beams have been used for validating the non-linear static analysis modeling procedure. Dimensional details are given in Table 8. The concrete compressive strength was 52 MPa. The yield strength for longitudinal reinforcement and shear reinforcement was 488 MPa and 328 MPa respectively. The beams were tested under 3 point bending. The modeling was done using the same procedure/approach as explained for previous validation example ($l_p=0.5d$; used cracked modulus of elasticity). The load vs mid span deflection responses are compared in Figure 28 and Figure 29, indicating good agreement.

Table 8 Dimensions of beams tested by Au & Bai [42]

Beam	L (mm)	L _o (mm)	b (mm)	h (mm)	d' (mm)	d (mm)	A _{st}	A _{sc}	Shear
B1	3000	2600	200	300	30	260	2-16Φ	2-12Φ	12Φ@175
B2	3000	2600	200	300	30	250	2-25Φ	2-12Φ	12Φ@175

L=Total length of beam; L_o=Effective span of beam; b= beam width; h=Depth of beam; d' = distance from extreme compression fiber to centroid of compression reinforcement; d = distance from extreme compression fiber to centroid of tension reinforcement; A_{st} = Tension reinforcement; A_{sc} = Compression reinforcement;

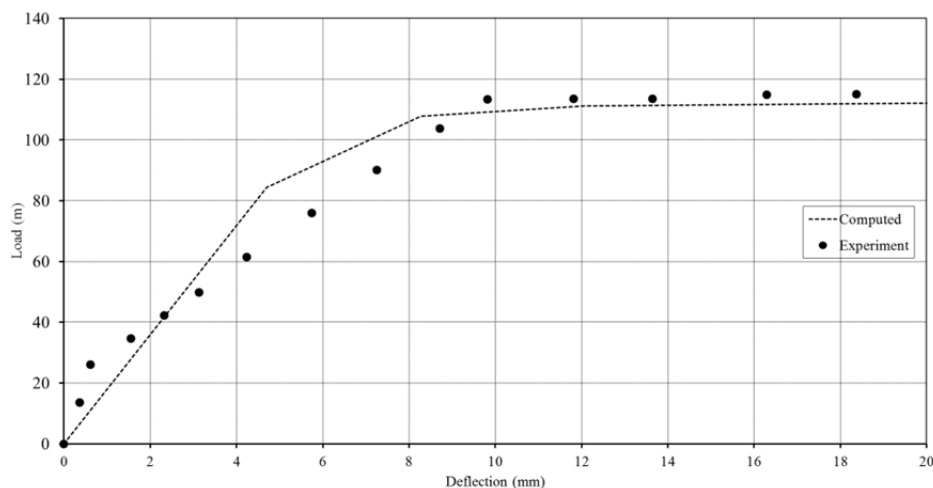


Figure 28 Load - deflection response for beam B1

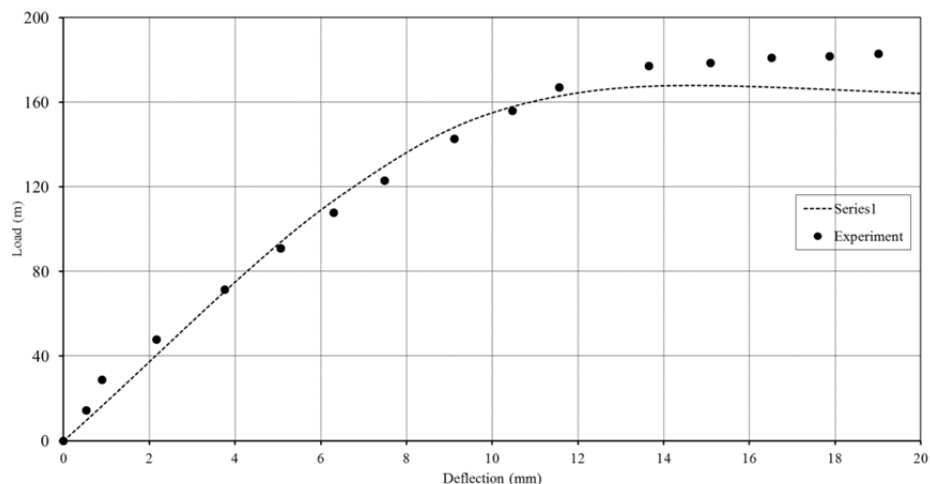


Figure 29 Load - deflection response for beam B2

4.3 Nonlinear Static Analysis Approach during fire

This section presents the validation of the proposed approach for conducting the nonlinear static analysis of flexural members during fire.

4.3.1 Beam I: Dotreppe [14]

Dotreppe [14] worked on numerical methods for simulation behaviour of RC members during fire. He reported two tests on full scale RC beams carried out at university of Ghent. The purpose of these tests was to determine the fire resistance of simply supported beams. Beams had a cross-section of 200 mm x 600mm and a span of 6500 mm. The beam was exposed to ISO 834 standard fire exposure until failure. Before fire exposure two point load of 65kN each were applied at the quarter points and was kept constant during fire. Figure 30 shows the beam section with reinforcement details. The compressive strength of concrete was not mentioned but permissible design compressive stress was given as 10MPa which corresponds to characteristic cube strength of 30 MPa ($f_c' = 24$ MPa). Experimentally obtained variation of yield strength and ultimate strength of reinforcing steel (cold worked) with temperature is shown in Figure 31.

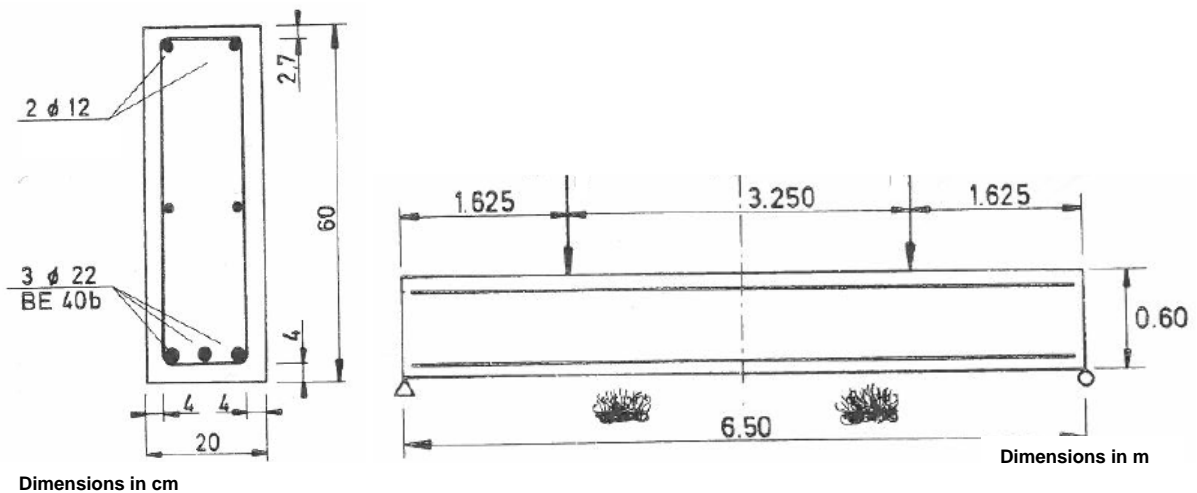


Figure 30 Reinforcement details of beams tested by Dotreppe [14]

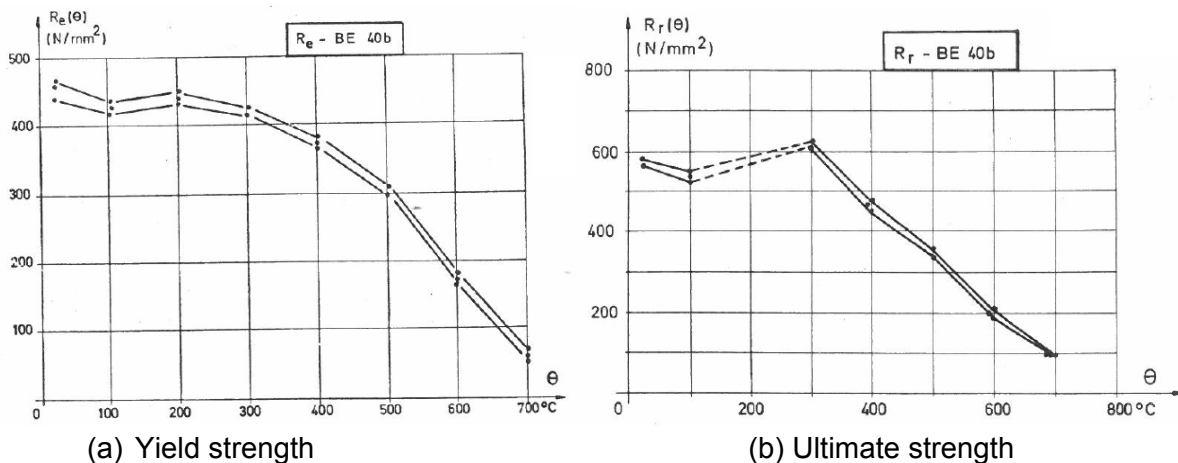


Figure 31 Variation of mechanical properties of reinforcing steel with temperature [14]

In step one, 2-D transient heat transfer analysis of the beam cross-section is performed. Figure 32 shows the temperature contour at regular time intervals of 15min. The computed and experimental temperature of central reinforcement bar in tension as shown in Figure 33; are in good agreement. The temperature predictions also match well with the FE simulation by Dotreppe & Franssen [43]. The initial rapid rise in temperature may be attributed to moisture migration, which has not been accounted in the present approach results in the initial difference.

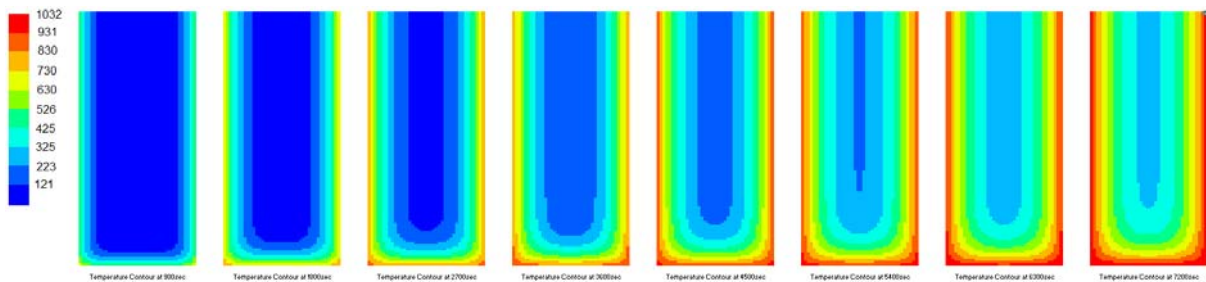


Figure 32 Predicted temperature contours under ISO834 standard fire

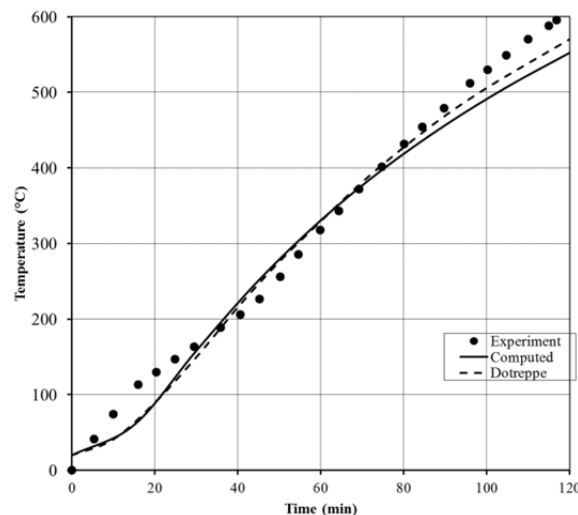


Figure 33 Comparison of temperature variation of central reinforcement

The second step is to compute the moment-curvature using the temperature gradients computed in step one. Computed moment-curvature relationships at every 15 min of 2hr fire exposure are shown in Figure 34. It can be seen that with increase in temperature the load carrying capacity of the member reduces but the curvature ductility increases:

These moment-curvature relationships are used in two ways. First these directly give us an estimate of fire rating based on strength (Limit state of strength). When the moment carrying capacity falls below the applied moment of 121.46 kN-m (including selfweight), the member fails. Hence, from Figure 34 the fire rating is computed to be 117min (7020 sec). Second these are used for computing the k_1 factor (Ref: Eqn. 21) for computing the stiffness parameter (Equivalent Modulus of Elasticity). k_1 factor accounts for reduction in stiffness due to material degradation and has been defined as the ratio of slope of linear region at particular time (of exposure) to slope at ambient temperature. Figure 35 shows the variation of k_1 factor for the beam under study.

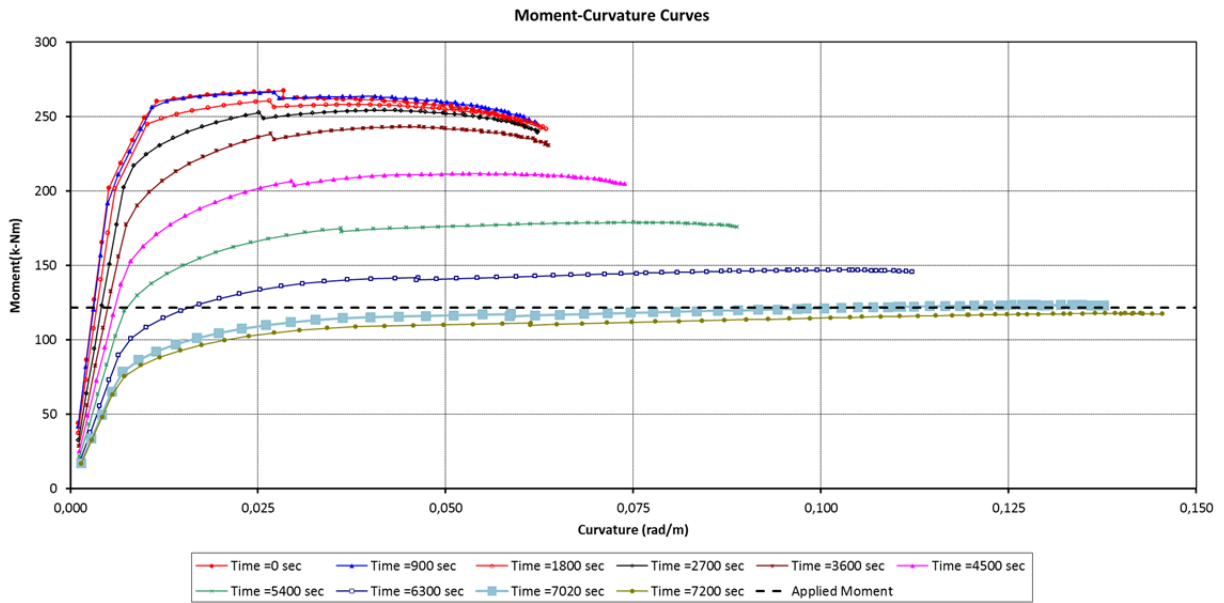


Figure 34 Moment curvature variation for Beam I

The third step is to perform nonlinear static analysis using the equivalent modulus of elasticity computed in Table 9 and the computed moment-curvature characteristics (Figure 34). These analyses are performed at each time which gives a family of load-displacement curves (Shown in Figure 36). Deflection – time curve is obtained by drawing a constant load line over the family of curves for load-deflection at various times as shown in Figure 36. The final comparison of computed deflection-time plot with the experimental results of two beams in Figure 37, shows a good agreement.

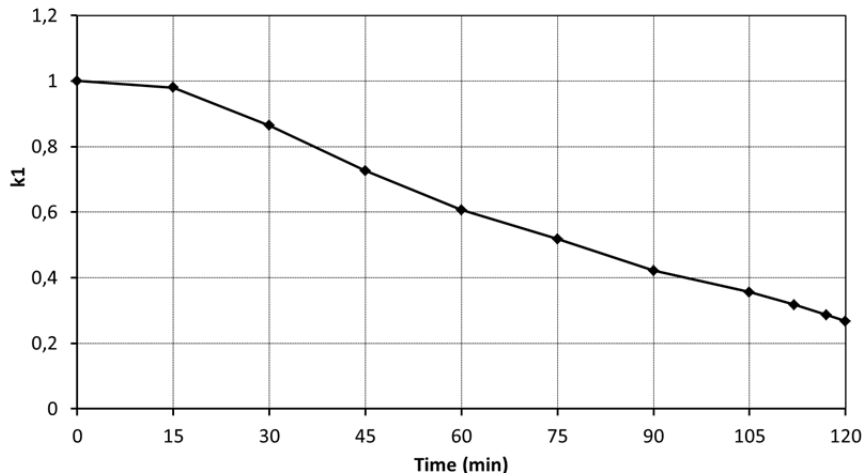


Figure 35 Variation of k_1 factor for Beam I

Table 9 Equivalent Modulus of Elasticity for Beam I

Time (min)	k_1	k_2	$E_{ct} = k_1 k_2 E_{cr}$
15	0.98	0.4	4514.04
30	0.86	0.4	3979.30
45	0.73	0.4	3346.27
60	0.61	0.4	2794.85
75	0.52	0.4	2356.45



90	0.42	0.4	1941.28
105	0.36	0.4	1640.81
112	0.32	0,4	1460.67
117	0.29	0.4	1318.97
120	0.27	0.4	1231.09

E_{cr} =Cracked modulus of elasticity at ambient temperature $(0.5 \times 4730(f'c)^{0.5})$

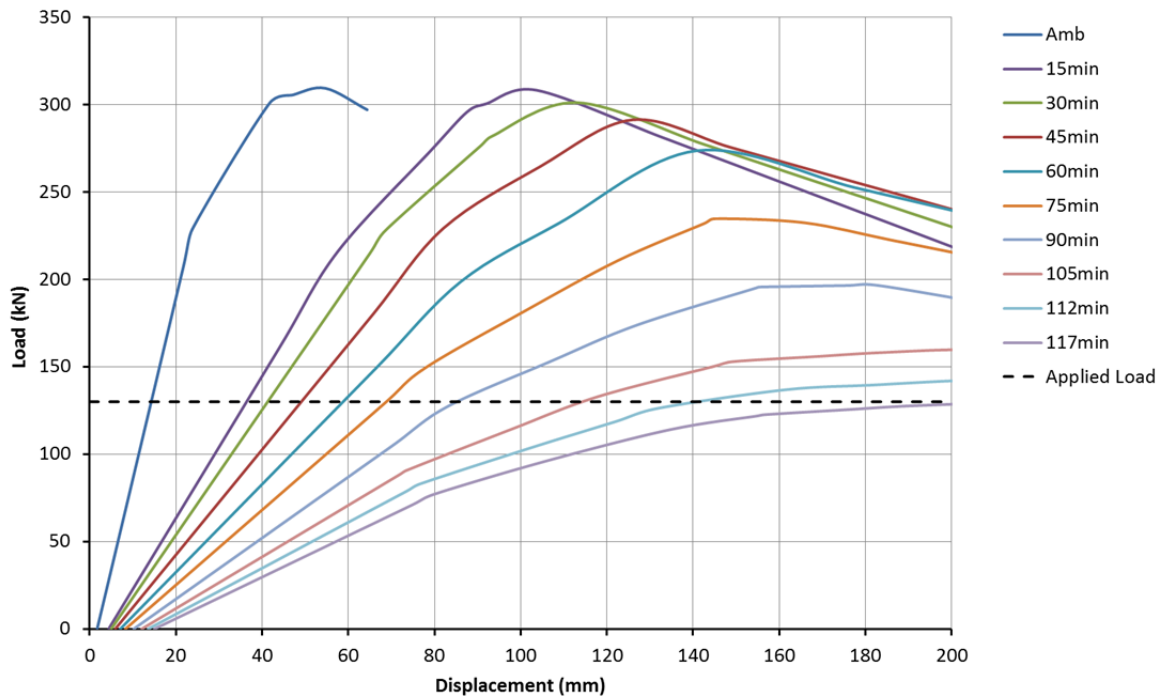


Figure 36 Load - deflection response at various time during fire exposure for Beam I

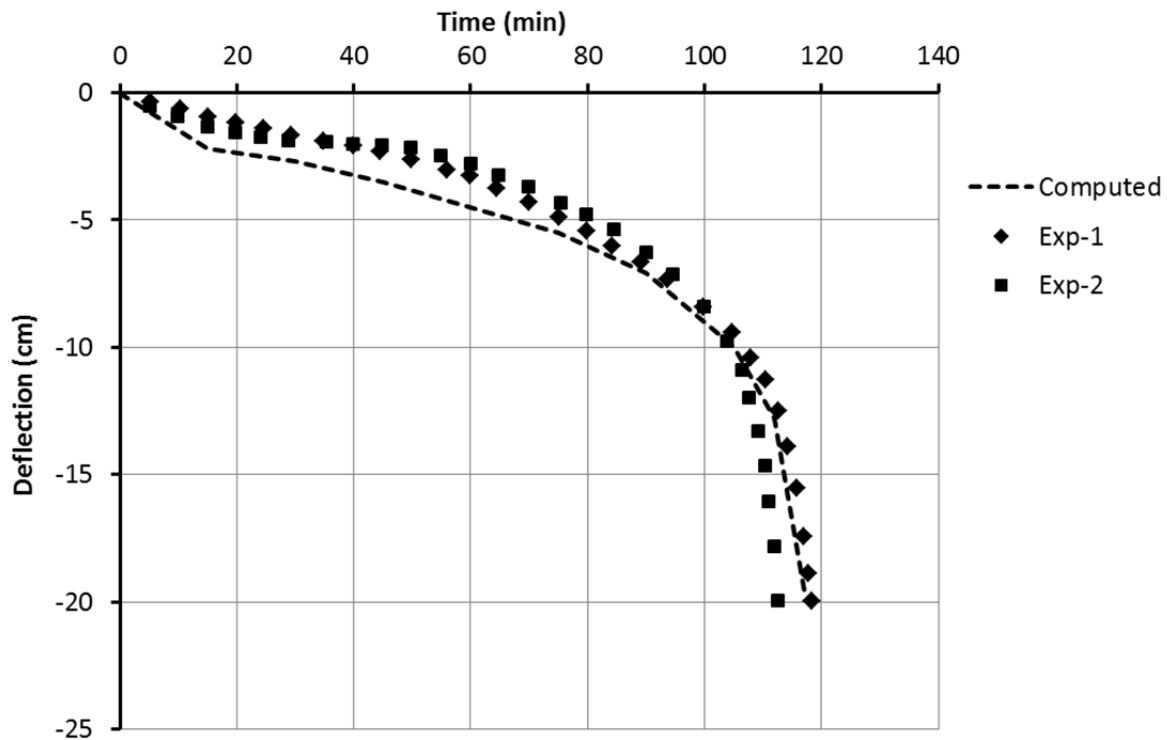


Figure 37 Deflection – time response comparison for Beam I

4.3.2 Beam II: Lin, Gustafsson and Abrams [15]

The test matrix consisted of 11 full scale RC beams under ASTM E119 standard fire exposure. The test program aimed to study/verify the effect of moment redistribution due to continuity. There was one beam, B-124 which was tested under simply supported condition as shown in Figure 38. The beam had a cross-section of 305 mm x 355 mm. The beams had a span of 6100 mm between the supports and cantilever of 1800 mm at both ends. The beam was loaded with 4 point loads equally distributed over the span between the supports. Each point load equal to 20kN, was applied before the fire exposure and was kept constant there after.

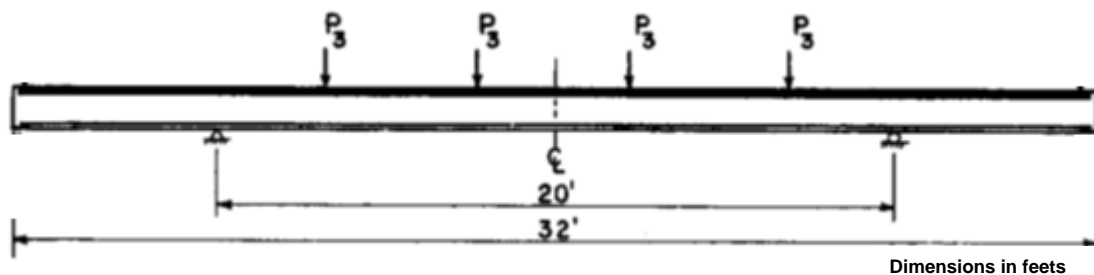


Figure 38 Loading arrangement for Beam II [15]

The tension reinforcement at mid span consists of 4-19Φ bars and the compression reinforcement was 2-19Φ bars. For shear reinforcement 9.5 dia bars @ 152mm centre to centre was provided. The reinforcement was assumed to be hot rolled. The measured average yield strength of longitudinal reinforcement was 435.8 MPa and the average cylinder strength for concrete on the day of testing was 30 MPa. Concrete was made of carbonate aggregate. The yield strength of shear reinforcement was 413.7 MPa (Grade60). The top and bottom clear cover to longitudinal reinforcement was 25mm and on the sides was 38mm. The test was terminated after 1hr 20 min of exposure but the beam has been analysed upto failure using the present approach demonstrated for Beam I. Figure 39 shows the lumped plasticity model for beam II prepared in SAP2000®.

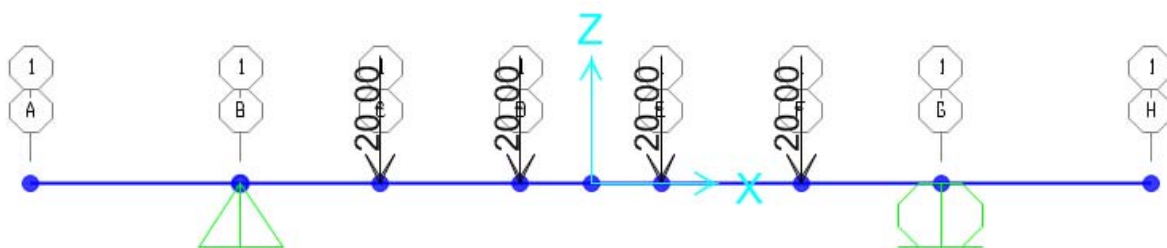


Figure 39 SAP2000 Model for Beam II

During test temperatures were recorded at various locations but only the average temperature of the bottom reinforcement was reported and has been compared in Figure 40. The computed temperature contours across the section at various time instances are shown in Figure 41.

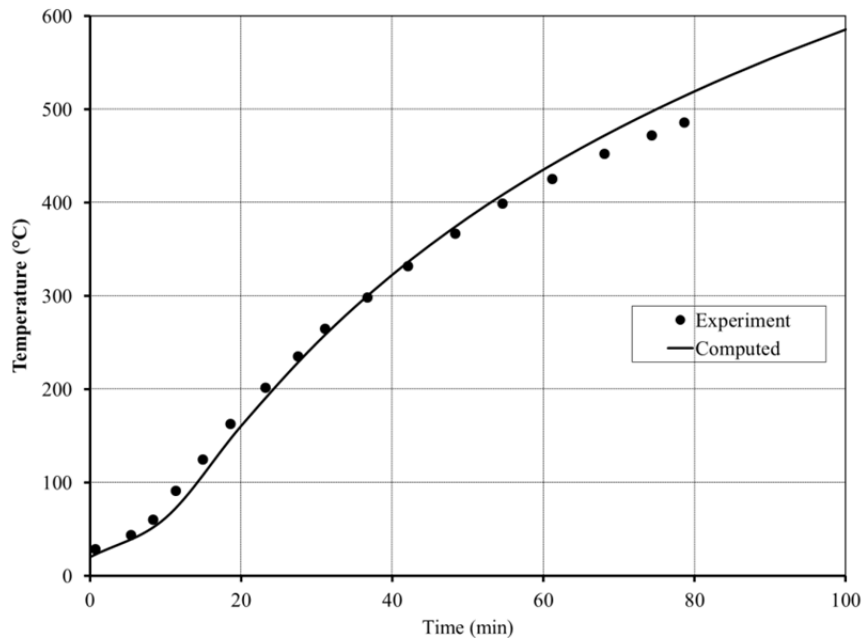


Figure 40 Average temperature of bottom reinforcement of Beam II

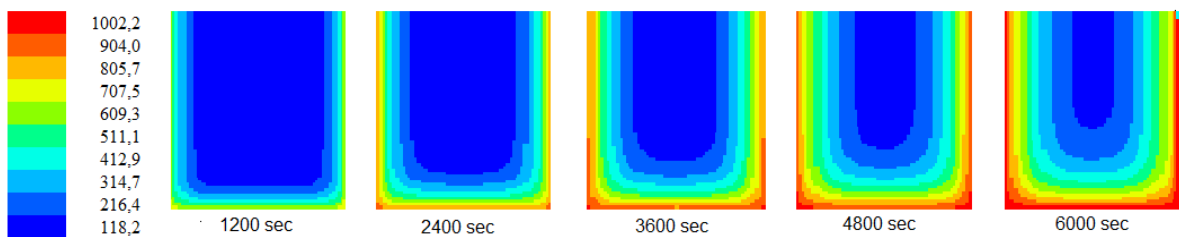


Figure 41 Predicted temperature contours for Beam II

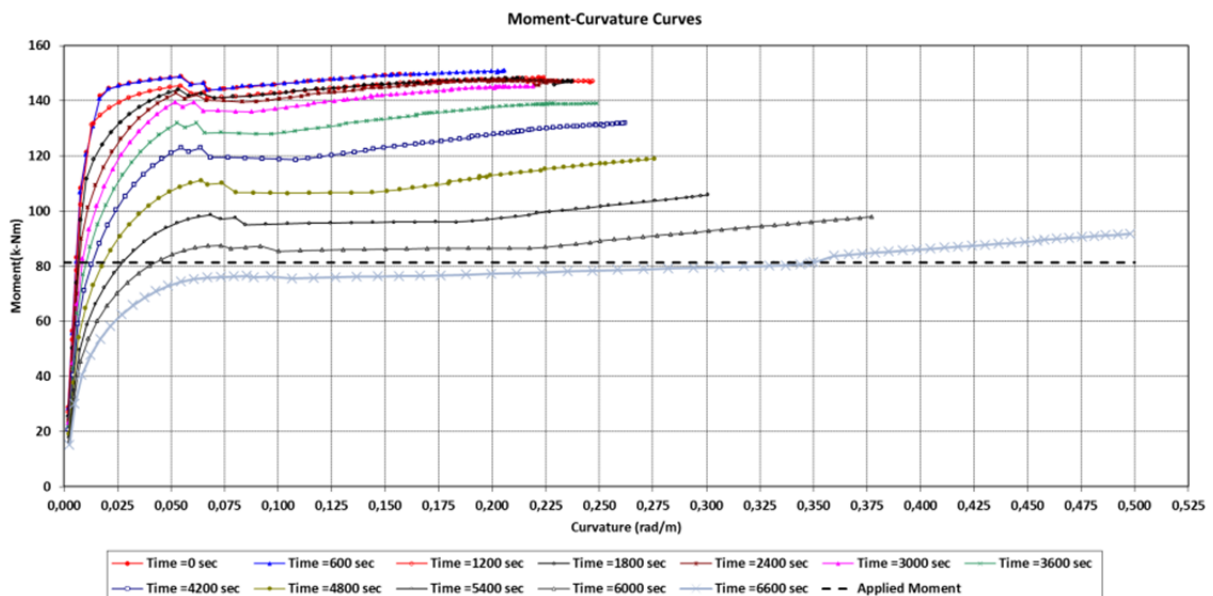


Figure 42 Moment curvature variation for Beam II

The computed moment-curvature curves with various exposure durations are shown in Figure 42. It can be observed that the beam fails in load carrying capacity at approx. 110 min. These computed moment-curvature characteristics were used to compute factor k_1 , which was used to obtain the equivalent modulus of elasticity, summarised in Table 10.



Using the above mentioned data nonlinear static analysis was performed at various time instances to obtain the corresponding load-deflection plots as shown in Figure 43. Since, the test was performed under constant load under standard fire, the experimental results were reported as time vs mid span deflection plot (Ref. Figure 44). Computed deflection-time plot is obtained by reading the deflections corresponding to the constant load line on Figure 43. Intersection of the constant load line of 80kN with load-deflection plots at various time instances corresponds to a point on the time – deflection plot. In this case also, the comparison between experimental result and the result obtained using the proposed approach, are in good agreement.

Table 10 Equivalent Modulus of Elasticity for Beam II

Time (min)	k_1	K_2	$E_{ct} = k_1 K_2 E_{cr}$
10	0.92	0.4	4713.14
20	0.87	0.4	4465.38
30	0.80	0.4	4126.93
40	0.72	0.4	3702.48
50	0.68	0.4	3489.24
60	0.55	0.4	2838.49
70	0.50	0.4	2555.47
80	0.44	0.4	2256.61
90	0.43	0.4	2229.85
100	0.38	0.4	1975.62
110	0.31	0.4	1618.30

E_{cr} =Cracked modulus of elasticity at ambient temperature $(0.5 \times 4730(f'c)^{0.5})$

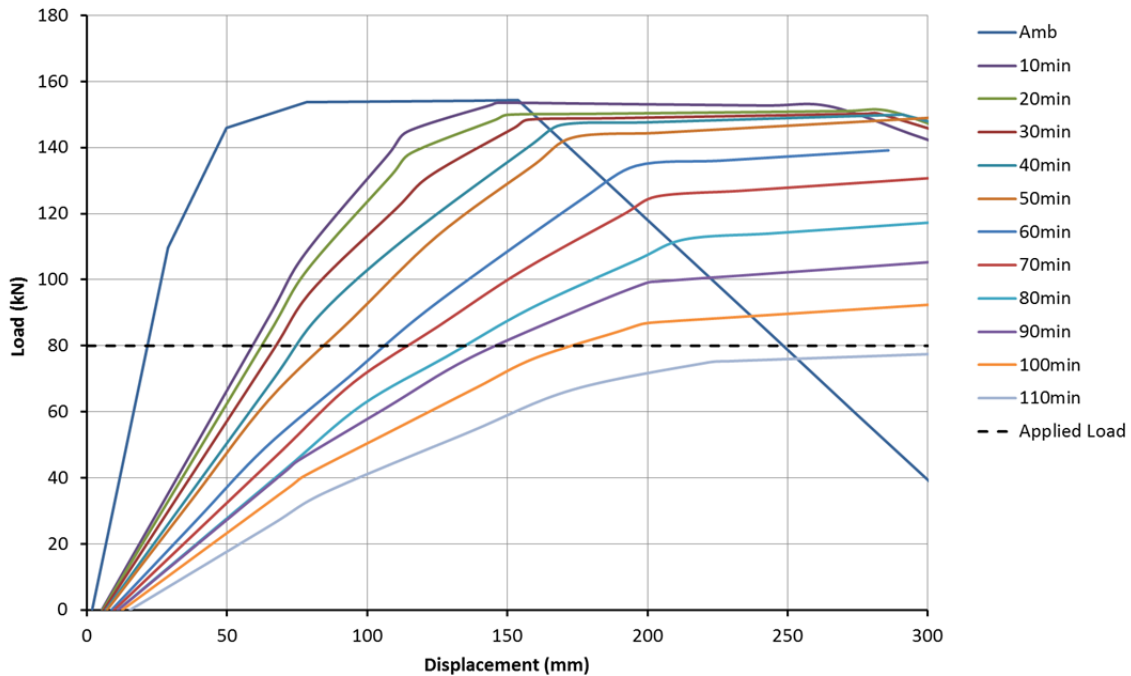


Figure 43 Load - deflection response at various time during fire exposure for Beam II

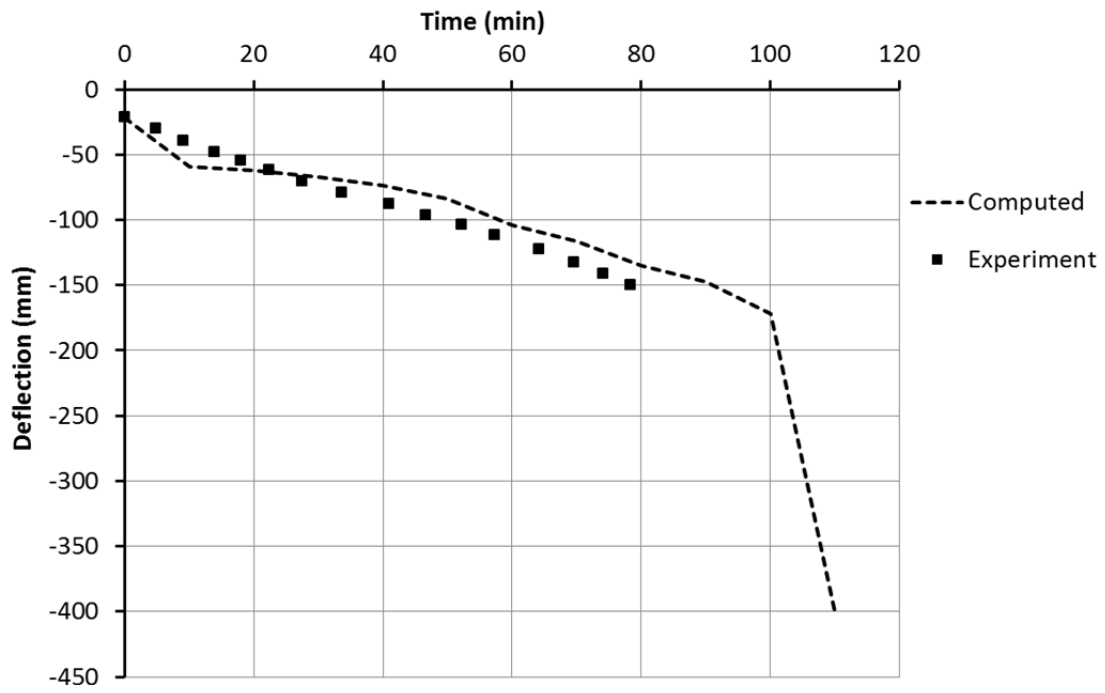


Figure 44 Deflection – time response comparison for Beam II



5 Summary and Conclusion

In this report, an analysis procedure to evaluate the structural performance of fire affected structural members is presented. The approach was earlier developed and validated [22] against the monotonic tests available in literature on RC beams after exposure to fire (residual state) to obtain the load-deflection response of the beams.

In this work, this approach is extended and applied to obtain the response of beams under constant load and exposed to fire loads in terms of deflection-time plots. The analysis procedure is validated against two tests on beams available in literature and excellent agreement between the experimental and analytical results is obtained for both the cases.

The analysis procedure consists of:

- (i) calculating temperature profiles across the section for fire exposure duration,
- (ii) calculating moment-curvature response of the section using temperature dependent constitutive laws for concrete and steel and the temperature gradients computed in step (i),
- (iii) performing nonlinear static analysis to obtain load-deflection response of the member and
- (iv) obtaining deflections-time response corresponding to the applied load from the series of load-deflection plots obtained in step (iii).

The report also discussed the in-house code developed for carrying out 2D transient heat transfer analysis and obtaining moment-curvature relationships. The module for computing moment-curvature characteristics has been successfully validated against two experiments available in literature.

The report also presents the validation of nonlinear static analysis procedure at ambient conditions against two experiments picked from literature. This validation was done to demonstrate the applicability of various assumptions. Hence, showing that, the various assumptions made during the implementation of this approach are reasonable.

The analysis is performed within the framework of lumped plasticity approach and can be used for practical and realistic analysis for fire performance assessment of fire affected structures.



6 Bibliography

1. Beitel JJ, Iwankiw NR, "Survey of multi story building collapses due to fire, fire resistance capabilities of test laboratories and research needs ", Third International workshop of Structures in Fire, 2004, Vol. , p. S1-1.
2. Buchanan AH, "Structural Design for Fire Safety" Chichester: Wiley, 2001.
3. Purkiss JA, "Fire Safety Engineering Design of Structures", 2nd ed.: Elsevier: Butterworth-Heinemann, 2007.
4. Drysdale D, "An Introduction to Fire Dynamics", 3rd ed.: Wiley, 2011.
5. SFPE , "Handbook of fire protection engineering", 3rd ed. Bethesda, Maryland: Society of Fire Protection Engineers, 2002.
6. Abrams MS, "Compressive strength of concrete at temperatures at 1600 °F ", Portland Cement Association, 1973, Vol. RD016.01T.
7. Schneider U, "Concrete at high temperatures: A general review ", Fire Safety Journal, 1988, Vol. 13, p. 55-68.
8. Cheng FP, Kodur VKR, Wang TC, "Stress strain curve for high strength concrete at elevated temperatures ", ASCE Journal of Materials in Civil Engineering, 2004, Vol. 16, Issue. 1, p. 84 - 90.
9. Anderberg Y, Thelandersson S, "Stress and deformation characteristics of concrete at high temperature, 2: Experimental investigation and material behaviour model ", Bulletin 54, 1976, Vol..
10. Diederichs U, Jumppanen UM, Penttala V, "Material properties of high strength concrete at elevated temperatures ", IABSE 13th Congress, 1988, Vol..
11. Takeuchi M, Hiramoto M, Kumagai N, Yamazaki N, Kodaira A, "Material properties of concrete and steel bars at elevated temperatures ", SMiRT - 12, 1993, Vol. , p. H04/4.
12. Castillo C, Durrani AJ, "Effect of transient high temperature on high strength concrete ", ACI Materials Journal, 1990, Vol. 87, Issue. 1, p. 47 - 53.
13. Sullivan PJE, Sharshar R, "Performance of concrete at elevated temperatures ", Fire Technology, 1992, Vol. 28, Issue. 3, p. 240 - 250.
14. Dotreppe JC. Numerical methods for the simulation of fire behavior of steel and reinforced concrete structures. (In French). University of Leige; 1980.
15. Lin TD, Gustaferro AH, Abrams MS, "Fire endurance of continuous reinforced concrete beams ", PCA R&D Bulletin RD072.01B, 1981, Vol..
16. Lin TD, Ellingwood B, Piet O, "Flexural and shear behaviour of reinforced concrete beams ", PCA R&D Bulletin, 1988, Vol. , p. RD091T.
17. Shi X, Tan TH, Tan KH, Guo Z, "Effect of force temperature paths on behaviours of reinforced concrete flexural members ", ASCE Journal of Structural Engineering, 2002, Vol. 128, Issue. 3, p. 365 - 373.
18. Shi X, Tan TH, Tan KH, Guo Z, "Influence of concrete cover on fire resistance of reinforced concrete flexural members ", ASCE Journal of Structural Engineering, 2004, Vol. 130, Issue. 8, p. 1225-1232.
19. Dwaikat MB, Kodur VKR, "Response of restrained concrete beams under design fire exposure ", ASCE Journal of Structural Engineering, 2009, Vol. 135, Issue. 11, p. 1408-



1417.

20. Choi EG, Shin YS, "The structural behaviour and simplified thermal analysis of normal strength and high strength concrete beams under fire ", Engineering Structures, 2011, Vol. 33, p. 1123 - 1132.
21. CEB-Fib Bulletin 46 , "Fire design of concrete structures - Structural behaviour and assessment ", Federation Internationale du beton (fib), 2008, Vol..
22. Lakhani H, Singh T, Sharma A, Reddy GR, Singh RK, "Prediction of post fire loa deflection response of RC flexural members using Simlistic Numerical Approach ", Structural Engineering and Mechancis, 2014, Vol. 50, Issue. 6, p. 755-772.
23. Lienhard IV JH, Lienhard V JH, "A Heat Transfer Textbook", 4th ed. Cambridge, Massachusetts: Phlogiston Press, 2015.
24. Park R, Paulay T, "Reinforced Concete Structures": John Wiley & Sons, 1975.
25. Eurocode2 , "Design of concrete structures - Part 1-2: General rules - Structural fire design" Brussels: European Committee For Standardization, 2004.
26. Youssef MA, Moftah M, "Genral stress strain relationship for concrete at elevated temperatures ", Engineering Structures, 2007, Vol. 29, p. 2618-2634.
27. Lakhani H, Kamath P, Bhargava P, Sharma UK, Reddy GR, "Thermal analysis of reinforced concrete structural elements ", Journal of Structural Fire Engineering, 2013, Vol. 4, Issue. 4, p. 227-243.
28. Kent DC, Park R, "Flexural members with confined concrete ", Journal of Engineering ASCE, 1971, Vol. 97, Issue. ST7, p. 1969-1990.
29. Mander JB, Priestley MJN, Park R, "Theoretical Stress-Strain model for confined concrete ", Journal of Structural Engineering, ASCE, 1988, Vol. 114, Issue. 8, p. 1804-1826.
30. Mander JB, Priestley MJN, Park R, "Observed stress strain behaviour of confined concrete ", Journal of Structural Engineering, 1988, Vol. 114, Issue. 8, p. 1827-1849.
31. Sharma A, Reddy GR, Elighausen R, Vaze KK, "Experimental and analytical investigation on seismic behaviour of RC framed structures ", Structural Engineering and Mechanics, 2011, Vol. 39, Issue. 1, p. 125-145.
32. Li L, Purkiss JA, "Stress strain constitutive equations of concrete material at elevated temperatures ", Fire Safety Journal, 2005, Vol. 40, p. 669 - 686.
33. Scott BD, Park R, Priestley MJN, "Stress strain behaviour of concrete confined by overlapping hops at low and high strain rates ", ACI Journal, 1982, Vol. 79, Issue. 1, p. 13 - 27.
34. Hertz KD, "Concrete Strength for fire safety design ", Mag. Concrete Res., 2005, Vol. 57, Issue. 8, p. 445 - 453.
35. Terro MJ, "NUmerical modeling of behaviour of concrete structures in fire ", ACI Structural Journal, 1998, Vol. 95, Issue. 2, p. 183 - 193.
36. ACI 318-14 , "Building code requirements for reinforced concrete" Detroit, Michigan: American Concrete Institute, 2014.
37. Applied Technology Council , "Improvement of nonlinear static seismic analysis procedures" Washington DC: Report No FEMA-440, 2005.
38. Expion B, Halleux P, "Moment curvature relationships of reinforced concrete sections under combined bending and normal force ", Materials and Structures, 1988, Vol. 21, p.



341 - 351.

39. Srikanth M, Kumar GR, Giri S, "Moment curvature of reinforced concrete beams using various confinement models and experimetnal validation ", Asian Journal of Civil Engineering (Building and Housing), 2007, Vol. 8, Issue. 3, p. 247 - 265.
40. Pam HJ, Kwan AKH, Islam MS, "Flexural strength and ductility of reinforced normal and high strength concrete beams ", Proceedings of the Institute of Civil Engineers, Structures & Buildings, 2001, Vol. 146, Issue. 4, p. 381 - 389.
41. Paulay T, Priestley MJN, "Seismic design of reinforced concrete and masonry buildings" New York: John Wiley and Sons, 1992.
42. Au FTK, Bai ZZ, "Two dimensional nonlinear finite element analysis of monotonically and non-reversed cyclicly loaded RC beams ", Engineering Structures, 2007, Vol. 29, p. 2921 - 2934.
43. Dotreppe JC, Franssen JM, "The use of nuerical models for the fire analysis of reinforced concrete and composite structures ", Engineering Analysis, 1985, Vol. 2, Issue. 2, p. 67 - 74.